Investigation of Novel Therapies for Hyperammonemia

Thesis

ANGELA DE ANGELIS

Investigation of novel therapies for hyperammonemia.

Ph.D. Thesis

The Open University

Affiliated Research Centre:

Telethon institute of Genetics and Medicine (TIGEM)

Director of Studies: Prof. **Nicola Brunetti-Pierri**

Thesis submitted in accordance with the requirements of

The Open University for the degree “Doctor of Philosophy”

September 2019

Table of Contents

Abstract

Ammonia is a toxic compound daily produced and consumed during cell metabolism in the body. It is converted to the less toxic substance urea by the urea cycle in the liver. Moreover, the urea cycle operates anatomically and functionally in sequence with the hepatic glutamine synthetase (GS) to detoxify ammonia and both systems are required for ammonia homeostasis. Urea cycle or GS deficiencies and liver diseases lead to defective ammonia removal causing hyperammonemia. Hyperammonemia is a life-threatening condition which may results in hepatic encephalopathy and death, if left untreated. Available therapies for hyperammonemia are partially effective and novel and improved therapies are required. Considering the cooperative role of GS in ammonia detoxification, gene therapy based on hepatic GS augmentation was investigated as a potential treatment against hyperammonemia. Thus, upregulation of hepatic GS protects wild-type mice against acute hyperammonemia. Notably, liver specific GS overexpression improved ammonia detoxification also in *Cps1*-deficient mice. As a result, hepatic GS augmentation therapy has potential for treatment of both primary and secondary forms of hyperammonemia.

Furthermore ammonia can induce modification of O-GlcNAcylation levels. O-GlcNAcylation is a dynamic post-translational modification catalyzed by the enzyme O-GlcNAc transferase (OGT) whereas the O-GlcNAcase (OGA) removes O-GlcNAc. O-GlcNAcylation, once modulated, may be a new therapeutic target to treat hyperammonemia. Hence, the role of hepatic O-GlcNAcylation in ammonia detoxification was investigated. *In vivo* modulation of O-GlcNAcylation through both pharmacological (small molecules) and OGA *knockdown* approaches improved ammonia detoxification. Neither expression of genes encoding urea cycle enzymes nor protein levels of these enzymes were affected by OGA inhibition, suggesting that

hepatic O-GlcNAcylation regulates ammonia clearance capacity by enzymatic activity of the urea cycle. Finally, hepatic O-GlcNAcylation plays an important role in ammonia detoxification. Therefore OGA is a novel therapeutic target for treatment of hyperammonemia of both urea cycle disorders and acquired hyperammonemia.

List of abbreviations

AAV: Adeno-associated virus

AFP: Alpha-fetoprotein

ATP: adenosine triphosphate

AU: arbitrary units

BUN: blood urea nitorgen

CoA: coenzyme A

CPSI: carbamoyl phosphate synthetase I

GLUL: glutamate-ammonia ligase (gene name)

GS: glutamine synthetase

G6PD: Glucose-6-phosphate dehydrogenase

HAT-like: histone acetyltransferase-like domain

HBP: hexosamine biosynthetic pathway

HCO_3^-: bicarbonate

HDAd: helper dependent adenoviral vector

HE: hepatic encephalopathy

i.p.: intraperitoneal injection

i.v.: intravenous injection

mOGT: mitochondrial OGT

N_2: Molecular nitrogen

NAG: N-acetylglutamate/ N -Acetylglutamic acid

ncOGA: nucleocytoplasmic OGA

ncOGT: nucleocytoplasmic OGT

NH_3: ammonia

NH_4^+: ammonium ions

O-GlcNAc: O-GlcNAcylation

OGA: O-GlcNAcase

OGT: O-GlcNAc transferase PBS: phosphate buffered saline

PEPCK: promoter of phosphoenolpyruvate carboxykinase

Pi: post-injection

PPP: pentose phosphate pathway

PTM: post-translational modification

SD: standard deviation

SE: standard error

SIRT1: Sirtuin 1

sOGA: short OGA

sOGT: short OGT

TRP: tetratricopeptide repeats

UCD: Urea cycle disorders

UDP-GlcNAc: Uridine diphosphate GlcNAc

carboxylase

Vp: viral particles

Wt: wild-type

Introduction

Ammonia metabolism

Nitrogen -the most abundant component of the earth atmosphere- is reduced to ammonia (NH_3) by nitrogen-fixing bacteria before it can be utilized by humans [1]. Ammonia dissolved in water forms ammonium ions (NH_4^+) and is assimilated into amino acids and other nitrogen-containing molecules. At physiological plasma and intracellular pH values, ammonia is present in its ionized form (ammonium, NH_4^+, pKa: 9.15). The concentration of ammonium in normal human plasma is 11-50 µmol/L [1]. Free ammonium ions are continually produced and consumed during cell metabolism in the human body. Ammonia arises during the breakdown of nucleotides, polyamines and deamination of amino acids [2]. In addition, free ammonium ions are supplied by urease- producing urea-splitting bacteria in the gastrointestinal tract. The liver has a relevant role in maintaining normal ammonium metabolism through urea cycle and glutamine metabolism. In the liver both systems are required for ammonia detoxification [3], operating anatomically and functionally in sequence [4] (**Fig. 1**).

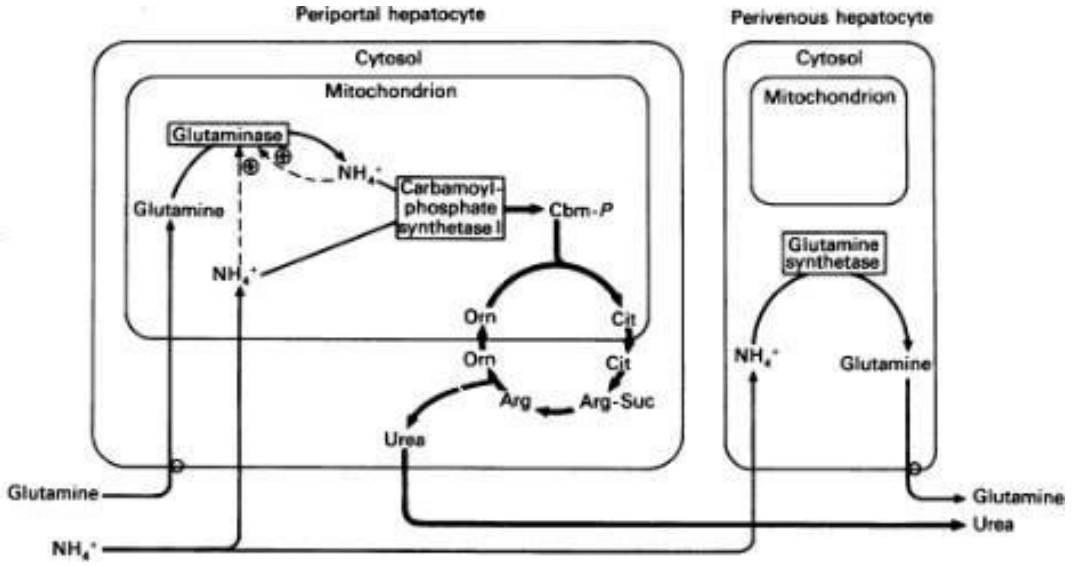

Figure 1. Organization of hepatic nitrogen metabolism (metabolic zonation). Periportal glutaminase is activated by ammonia and acts as ammonia amplifier. Its activity determines flux of ammonia through urea cycle, a low affinity system for ammonia detoxification. Glutamine synthetase in perivenous hepatocytes acts

as high affinity system for ammonia detoxification. Adapted from [3].

The urea cycle is a low-affinity and high capacity ammonia detoxification pathway occurring in periportal hepatocytes while glutamine synthetase (GS) in perivenous hepatocytes is a high-affinity ammonia scavenger system [3]. The urea cycle occurs only within the liver mitochondria and cytoplasm. The conversion from ammonia into urea involves five catalytic enzymes (carbamyl phosphate synthetase I, ornithine transcarbamylase, argininosuccinate synthase, argininosuccinate lyase, and arginase) and one enzyme that synthesizes an allosteric activator (N-acetylglutamate synthase) **(Fig. 2**). The initial steps of the urea cycle occurs in the mitochondria whereas the remaining three steps are cytosolic (**Fig. 2**).

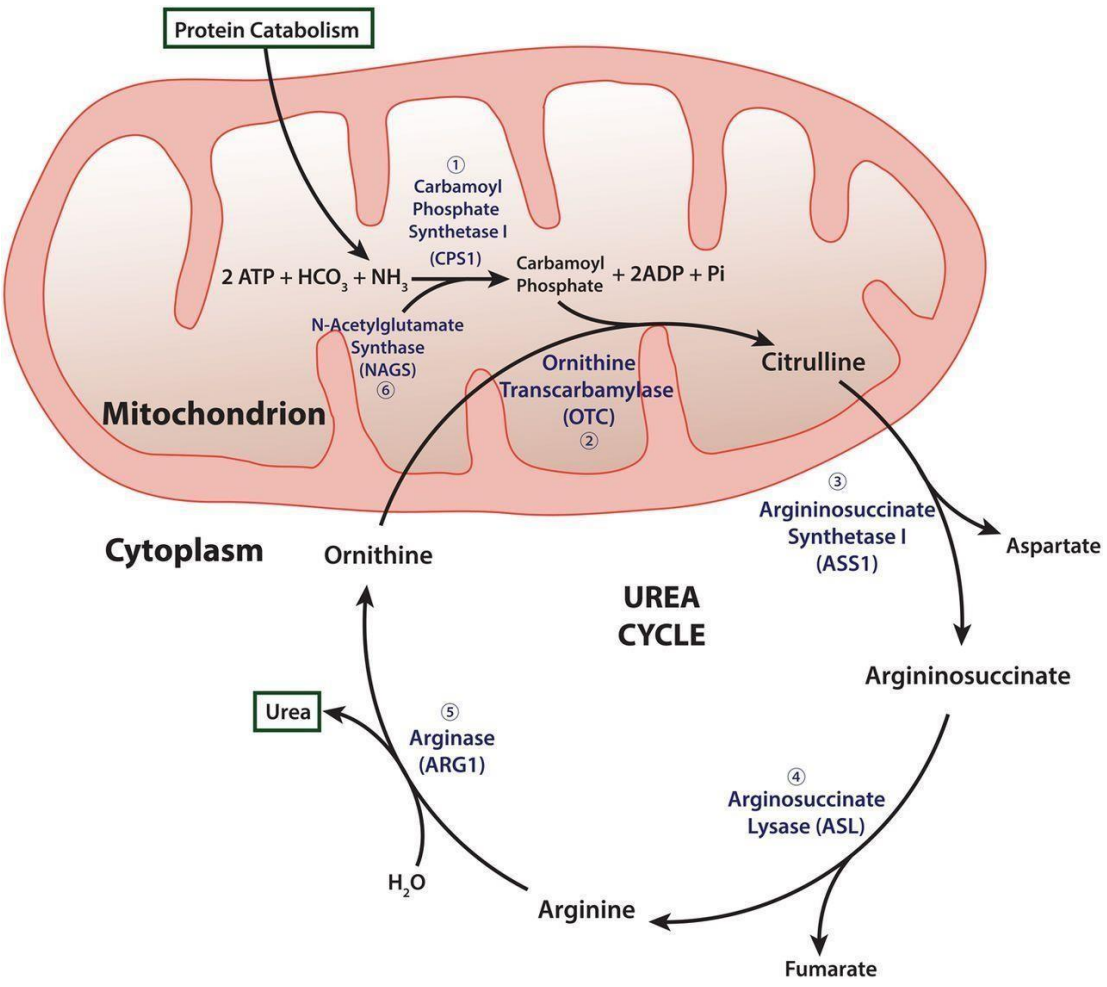

Figure 2. Schematic representation of urea cycle. The urea cycle is a metabolic pathway that converts highly toxic ammonia to urea which is nontoxic, highly soluble, and can rapidly be excreted by kidneys. Urea is formed from NH_4^+ (as derived from oxidative deamination of glutamate), HCO_3^-, the nitrogen of aspartate and ATP.

The conversion from ammonia to urea occurs through five reactions. The first and rate-limting step is needed for ammonia to enter the cycle in which ammonia is converted to carbamoyl phosphate. The following four enzymatic reactions are all a part of the cycle itself: one mitochondrial and three cytosolic. The synthesis of carbamoyl phosphate and the activity of urea cycle are dependent on the presence of N-acetylglutamic acid (NAG), which allosterically activates carbamoyl phosphate synthetase I (CPS1). The remaining enzymes of the cycle are controlled by the concentrations of their substrates. Adapted from [23].

GS, also known as glutamate-ammonia ligase enzyme (*GLUL*), is a cytosolic enzyme that incorporates an ammonia molecule into glutamate to form glutamine through an ATP-dependent reaction. It is highly conserved in living organisms and its expression and activity have been detected in several tissues including liver and brain (mostly astrocytes) [1]. Glutamine, the product of GS reaction, is the most abundant free amino acid in the human body and is crucial in essential pathways such as cell signaling, osmotic regulation, acid-base homeostasis and proliferation. Glutamine serves as a major nontoxic interorgan ammonia carrier [4].

Hyperammonemia: pathogenesis and treatments

Hyperammonemia is defined as a concentration of plasma ammonia level more than 50 µmol/L (> 100 µmol/L in newborns). It can occur when ammonia detoxification is deficient (decreased urea cycle flux, insufficient activity of GS) or under conditions with increased ammonia production (drugs, infections, intestinal bacterial overgrowth or other catabolic states leading to endogenous protein degradation) [5]. Depending on the underlying pathophysiology, hyperammonemia can be defined as primary and secondary. Primary hyperammonemia is caused by inborn errors of metabolism, mainly urea cycle disorders (UCD) that may be due to deficiency of any of the enzymes in the urea cycle. UCD are all autosomal recessive except ornithine transcarbamylase (OTC) deficiency which is X-linked. Deficiency of Carbamoyl phosphate synthetase I (Cps1) is typically very severe because it is due to a defect in the initial incorporation of ammonia into intermediate compounds of urea cycle [6]. In contrast, secondary hyperammonemia is a result of accumulation of any of toxic metabolites or substrate deficiencies of the urea cycle [5]. The most common examples of secondary hyperammonemia include organic acidemias in which urea synthesis is impaired by reduced production of N-acetylglutamate (NAG), the allosteric activator of ureagenesis through carbamoyl phosphate synthetase I [1; 7; 8]. Interestingly, similar to inherited urea cycle disorders, patients with ultra-rare genetic GS deficiency also show hyperammonemia [9; 10]. Furthermore, GS expression and its activity is reduced in patients with liver cirrhosis and chronic hyperammonemia [11] and in mice liver-specific deletion of GS results in hyperammonemia leading to neuronal and behavioural abnormalities [12]. As a result hyperammonemia occurs not only in UCD, congenital or acquired deficiency of any of the enzymes involved in the urea cycle disorders, but also in GS deficiency and in acute liver failure (sepsis and cirrhosis) [13]. Thus, also acquired impairment of the liver function leads to severe neurological disease. Consequently, an increase in the blood ammonia concentration leads to higher levels of ammonia in brain, eventually resulting in astrocyte swelling, increased blood-brain barrier permeability, altered cerebral metabolism and neurotransmission and cerebral edema [14].

Hyperammonemia can trigger hepatic encephalopathy (HE) a serious psychiatric and neurocognitive complication.

Therapeutic approaches for hyperammonemia aim at reducing production by protein-restriction diet and uptake of ammonia (antibiotics, probiotics non-absorbable disaccharides) or improving endogenous detoxification systems (ammonia scavenger drugs, e.g. phenylacetate and phenylbutyrate) [14]. Despite these treatments, patients remain at risk of acute decompensation and liver transplantation is often considered [15; 16]. However, liver transplantation is hampered by risks of mortality and morbidity, largely related to long-term effects of immunosuppression. Therefore, there is a need for developing novel and more effective therapeutic strategies to reduce ammonia levels and to decrease mortality and morbidity in individuals with hyperammonemia [14].

O-GlcNAcylation: mechanisms and functions

O-GlcNAcylation (O-GlcNAc) is a post-translational modification (PTM) consisting of non-canonical glycosylation with the attachment of a O-linked N-acetylglucosamine (O-GlcNAc) to serine and threonine residues of cytoplasmic, nuclear and mitochondrial proteins [17]. Uridine diphosphate GlcNAc (UDP-GlcNAc) is the substrate of O-GlcNAc and it derives from the hexosamine biosynthetic pathway (HBP) which integrates glucose, amino acids, fatty acids and nucleotide metabolism to generate UDP-GlcNAc (**Fig. 3**).

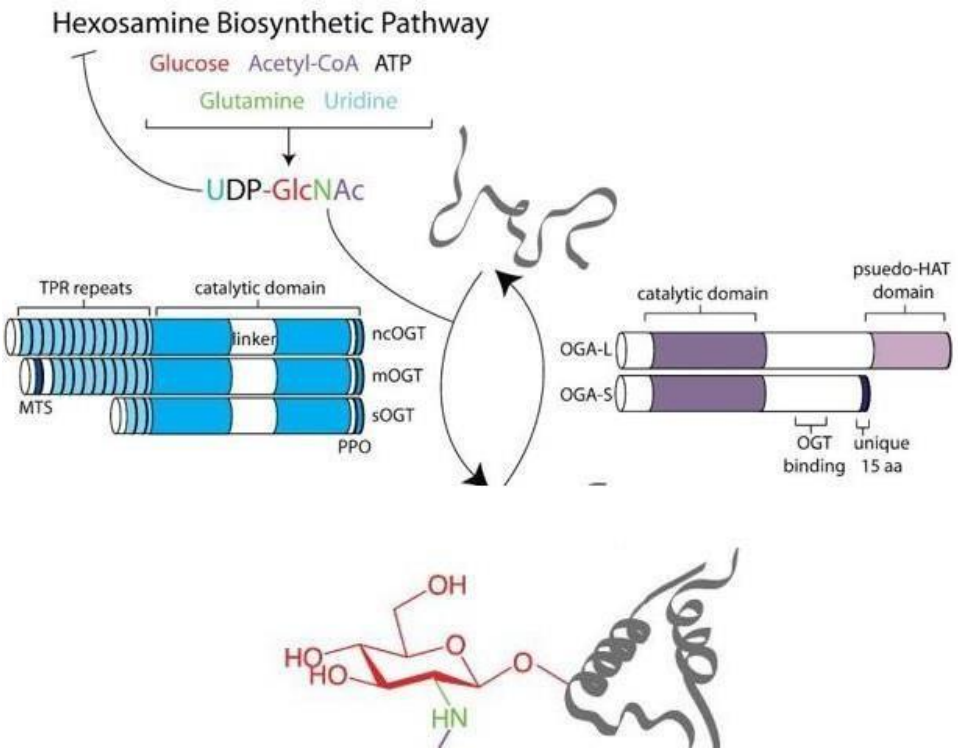

Figure 3. Dynamic, nutrient-sensitive O-GlcNAc cycling is modulated by metabolite and enzyme availability. Glucose, acetyl-CoA, ATP, glutamine, and uridine are required for synthesis of UDP-GlcNAc, the ultimate product of the hexosamine biosynthetic pathway (HBP). hOGT and hOGA splice variants are depicted. O-GlcNAc transferase (OGT) uses the nucleotide sugar to modify proteins, whereas O-GlcNAcase (OGA) catalyzes the removal of GlcNAc. Abbreviations: HAT: histone acetyltransferase; MTS, mitochondrial targeting sequence; PPO, phosphoinositide binding domain; TRP: tetratricopeptide repeats. Adapted from [22].

The attachment of the sugar is catalyzed by O-GlcNAc transferase (OGT) transferring a O-GlcNAc moiety from the donor substrate UDP-GlcNAc to the hydroxyl groups of serine

and threonine residues; whereas O-GlcNAcase (OGA) is responsible for the removal of the sugar modification. OGT and OGA are the only two enzymes involved in the regulation of this PTM. There are multiple isoforms of OGT and OGA. Based on splicing of amino-terminal tetratricopeptide repeats (TRPs), there are three isoforms of OGT: nucleocytoplasmic (ncOGT), mitochondrial (mOGT) and short (sOGT) that share common carboxy-terminal catalytic and phosphoinositide binding domains and differ for their subcellular localization. Moreover, OGA presents two isoforms: a nucleocytoplasmic isoform (ncOGA), which possesses both an N-terminal O-GlcNAc hydrolase domain and a C-terminal histone acetyltransferase-like domain (HAT-like) and a short isoform (sOGA), lacking HAT-like domains. O-GlcNAcylation interacts extensively with other PTMs especially with phosphorylation. O-GlcNAcylation occurs reciprocally or sequentially with phosphorylation on the same residues of several proteins [18;19] and it is thought that these two PTMs are in a dynamic equilibrium [20]. Like phosphorylation, O-GlcNAcylation is a dynamic modification and can be transferred to, and removed from, a protein many times during the lifespan of a protein [20]. While phosphorylation is controlled by a cascade of kinases and phosphatases, O-GlcNAcylation is regulated only by two enzymes, namely OGT and OGA. Similar to phosphorylation, O-GlcNAcylation strongly affects protein functions, such as catalytic activity or protein-protein interactions [21]. O-Glc-NAcylation targets include transcription factors and proteins involved in histone modifications, DNA methylation and intracellular signaling [22] **(Fig. 4**). Moreover, this PTM has been implicated in several metabolic pathways in liver such as carbohydrate and lipid metabolism, circadian clock, mitochondrial functions and autophagy [17]. Reversible protein O-GlcNAcylation was found to be induced by ammonia treatment in rat astrocytes suggesting that O-GlcNAcylation is involved in the pathophysiology of hepatic encephalopathy [21].

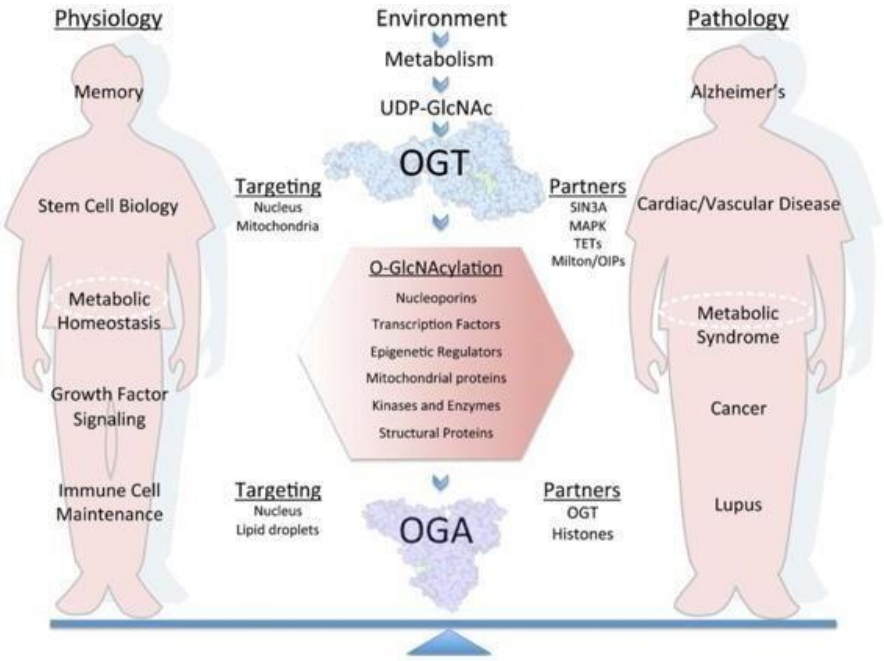

Figure 4: Role of O-GlcNAcylation in human physiology and pathology states. The ubiquitous and essential modification of protein serine and threonine residues with O-GlcNAc modulates cell functions by responding to variable nutrient conditions. Aberrant O-GlcNAc modification is implicated in metabolic and neurodegenerative diseases, cancer, and autoimmune disorders. Abbreviations: OIP, OGT interacting protein. Adapted from [22].

Aims of the thesis

Hepatic GS augmentation and pharmacologic modulation of O-GlcNAcylation: new therapeutic approaches for hyperammonemia

The goal of the thesis work was to investigate novel therapies for treatment of hyperammonemia by two independent studies. Recent findings suggested that enhancement of GS expression in muscle has therapeutic potential for treatment of hyperammonemia [15]. Moreover, increased activity of muscle GS induced by ornithine-phenylacetate treatment was found to reduce blood ammonia in rat models of chronic liver failure [13]. Based on these findings, I investigated the efficacy of hepatic GS overexpression for therapy of hyperammonemia. For a proof-of-concept study, I used an approach based on liver-directed gene transfer of GS (**Aim 1**).

In **aim 2** of this thesis, I investigated the relationship between O-GlcNAcylation and ammonia. Starting from the observation made in our laboratory that O-GlcNAcylation is an ammonia-induced PTM [21], I hypothesized that O-GlcNAcylation might be a novel therapeutic target for treatment of hyperammonemia.

In summary, the main purpose of my thesis is to study novel and effective therapeutic approaches to treat hyperammonemia and towards this goal, I investigated :

1. the efficacy of hepatic GS supply in reducing hyperammonemia induced in acute and chronic models.
2. the efficacy of pharmacologic modulation of O-GlcNAcylation on improving ammonia detoxification capacity.

Results

AIM 1: Hepatic GS overexpression for therapy of hyperammonemia

To investigate the potential of hepatic GS augmentation as a therapeutic approach for hyperammonemia, a helper dependent adenoviral vector (HDAd) expressing the murine glutamine synthetase under the control of a liver-specific expression cassette (HDAd-GS) was generated (**Fig. 5A**). HDAd can efficiently deliver genes to hepatocytes to provide long-term, high-level transgene expression without inducing chronic toxicity [25] and have been used in a variety of inherited liver diseases [27;29;30]. It has long been appreciated that hepatocyte gene therapy using HDAd, the latest generation of recombinant vectors, mediates high level transgene expression with negligible chronic toxicity, as shown by several studies in small and large animal models [24;25; 26; 27; 28]. The helper dependent adenoviral vector was produced to express murine glutamine synthetase under the control of the liver-specific promoter of phosphoenolpyruvate carboxykinase (PEPCK). Firstly, C57BL/6 wild-type mice were injected with HDAd-GS or HDAd-AFP encoding the unrelated nontoxic, non immunogenic alpha-fetoprotein (AFP) reporter gene under the control of the same liver-specific expression cassette. Compared to C57BL/6 wild-type control mice injected with HDAd-AFP, increased hepatic GS protein expression levels was observed in C57BL/6 wild-type injected with the vector expressing GS by western blot (**Fig. 5B**).

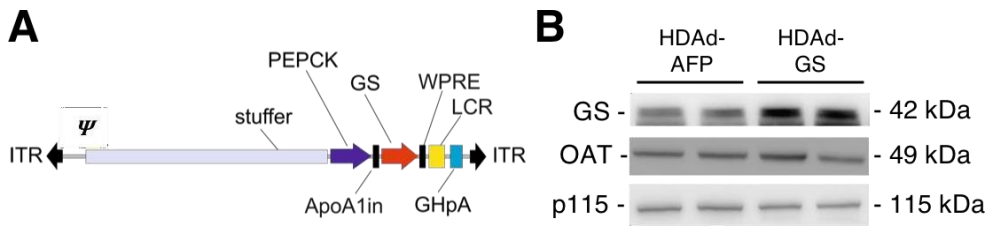

Figure 5. (A) A helper-dependent adenoviral vector was produced to express murine GS under the control of the phosphoenolpyruvate carboxykinase (PEPCK) promoter. The vector also contains inverted terminal repeat (ITR), a packaging signal (Ψ), the ApoA1 intron (ApoA1in), the hepatic locus control region (LCR),

a growth hormone polyadenylation signal (GHpA) and woodchuck hepatitis post-transcriptional regulatory element (WPRE). **(B)** Western blot of GS in livers of HDAd- GS-injected C57BL/6 wild-type mice compared to controls injected with a vector expressing an unrelated reporter gene (HDAd-AFP) at 12 weeks post vector injection. Ornithine aminotransferase (OAT) and p115 were used as loading controls. Band densitometric densities of HDAd-AFP: 1.00 ± 0.05 AU [arbitrary unit] vs HDAd-GS: 1.88 ± 0.20 AU; P = 0.022, two-tailed unpaired Student's t test; n = 3/group.

These wild-type mice injected with HDAd-GS or HDAd-AFP were treated intraperitoneally with ammonium chloride (NH_4Cl) at the dose of 10 mmol/kg. Serum ammonia levels did not change at baseline but mice with hepatic GS upregulation showed a 39% reduction in serum ammonia at 0.5 hours after i.p. ammonium chloride challenge compared to controls ($P < 0.05$; **Fig. 6A**). A concomitant increase in serum levels of glutamine (the product of the GS reaction) occurred in mice with hepatic GS overexpression compared to HDAd-AFP-injected controls (**Fig. 6B**), whereas serum urea was unaffected (**Fig. 6C**).

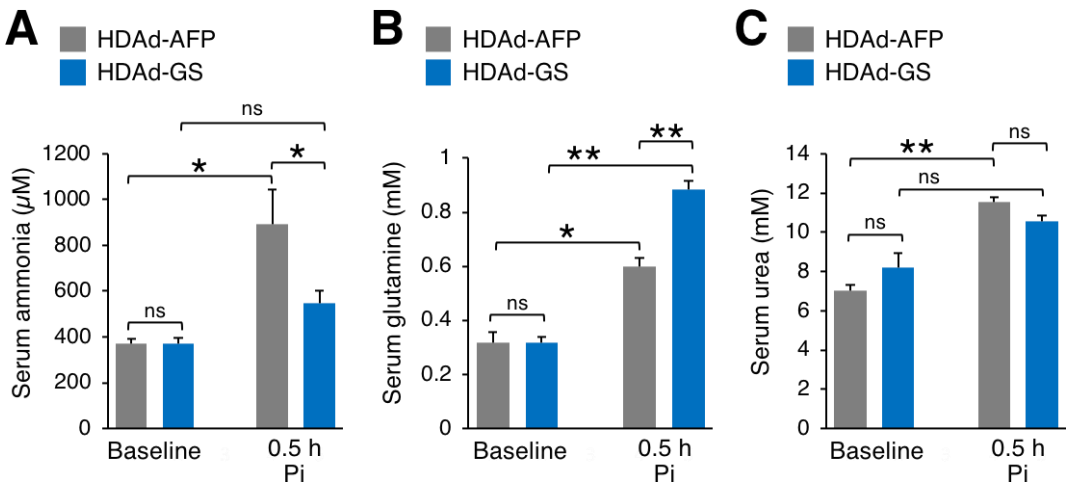

Figure 6. Upregulation of hepatic GS protects wild-type mice against acute hyperammonemia. **(A-C)** Serum ammonia, glutamine, and urea at baseline and 0.5 hours after intraperitoneal injections of ammonium chloride (10 mmol/kg) in wild-type mice injected with HDAd-GS or HDAd-AFP vector. (n ≥ 9/group). *P < 0.05; **P <

0.01. Abbreviations: AFP: α-fetoprotein; GS: glutamine synthetase; HDAd: helper-dependent adenoviral vector; Pi: post injection.

These results suggested that liver-specific GS overexpression improved ammonia detoxification through an increase in hepatic glutamine synthesis in wild-type mice with acute hyperammonemia.

To investigate whether increased hepatic GS expression is effective for therapy of hyperammonemia due to UCD, mice with deficiency of CPS1 were next injected with HDAd-GS or HDAd-AFP. CPS1 is the initial and rate-limiting step of urea cycle that forms carbamoyl phosphate from bicarbonate, ammonia and ATP. Bi-allelic mutations of *Cps1* result in a UCD presenting with hyperammonemia, often with reduced citrulline and without orotic aciduria. CPS1 deficiency is a particularly challenging disorder because it lacks early recognition signs and typically results in early neonatal death. Moreover, therapeutic interventions have limited efficacy and most patients develop long-term neurologic sequelae.

These experiments were performed in collaboration with Dr. Gerald S. Lipshutz (UCLA, Los Angeles, California, USA) using Cre-mediated conditional hepatic deficient mouse for *Cps1* generated in his laboratory to overcome the early lethality of mice deficient in CPS1 enzyme [31]. Deletion of the *Cps1* locus was achieved in adult transgenic $Cps1^{tm1c/tm1c}$ mice by i.v. injection of a low dose of serotype 8 adeno-associated viral vector (AAV8) expressing the Cre recombinase inducing non lethal increase in plasma ammonia [32]. This conditional murine model recapitulates the clinical and biochemical phenotype of human patients with *CPS1* deficiency. As a result, Cre- mediated reduction in hepatic *Cps1* mRNA levels was similar in mice injected with HDAd expressing either AFP or GS (**Fig. 7**).

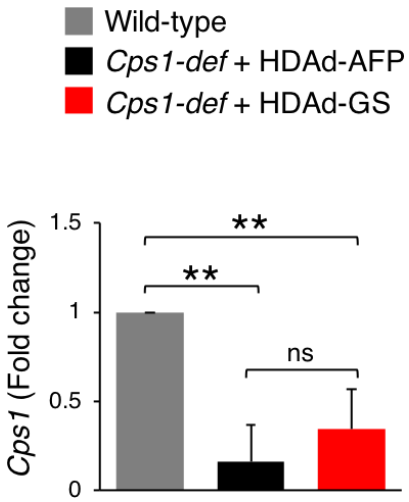

Figure 7. Expression of *Cps1* gene in HDAd-GS and HDAd-AFP injected mice. *Cps1* mRNA expression in Cre-mediated *Cps1*-deficient (*Cps1-def*) mice injected with HDAd-GS or HDAd-AFP compared to control wild-type animals (n = 5/group). **p< 0.01 (One-way ANOVA). Abbreviations: AFP: α-fetoprotein; GS: glutamine synthetase; HDAd: helper-dependent adenoviral vector; ns: not significant.

Similar reduction of CPS1 levels in mice expressing either AFP or GS when compared to wild-type mice was shown by immunofluorescence performed on livers with anti-CPS1 antibody (**Fig. 8A**). Moreover, mice expressing either AFP or GS showed decreased blood urea nitrogen (BUN) compared to wild-type controls that was also similar among the two groups (**Fig. 8B**), confirming the urea cycle deficiency affecting *Cps1-def* mice.

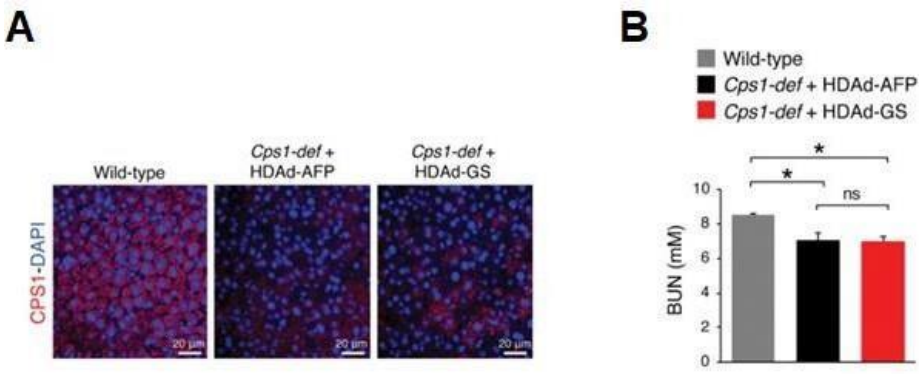

Figure 8. (A) Representative images of immunofluorescence microscopy for CPS1 (red) in livers harvested at day 28 post-vector administration in *Cps1-def* mice injected with HDAd-GS or HDAd-AFP compared to control wild-type animals. **(B)** BUN in plasma harvested at day 28 post vector administration in Cre-mediated *Cps1*-deficient (*Cps1-def*) mice injected with HDAd-GS or HDAd-AFP compared to control wild-type animals (n = 5/group). *$P < 0.05$ (one-way ANOVA). Data represent averages ± SEM. Abbreviations: AFP: α-fetoprotein; BUN: blood urea nitrogen; CPS1: carbamoyl phosphate synthetase 1. GS: glutamine synthetase; HDAd: helper-dependent adenoviral vector; ns: not significant.

As expected, livers of HDAd-GS-injected $Cps1^{tm1c/tm1c}$ mice showed increased GS expression compared to HDAd-AFP controls ($P < 0.01$; **Fig. 9A**). Interestingly, mice treated with HDAd-GS showed an increased plasma glutamine/ammonia ratio (**Fig. 9B**), suggesting that increased glutamine synthesis is responsible for the reduced blood ammonia levels induced by HDAd-GS.

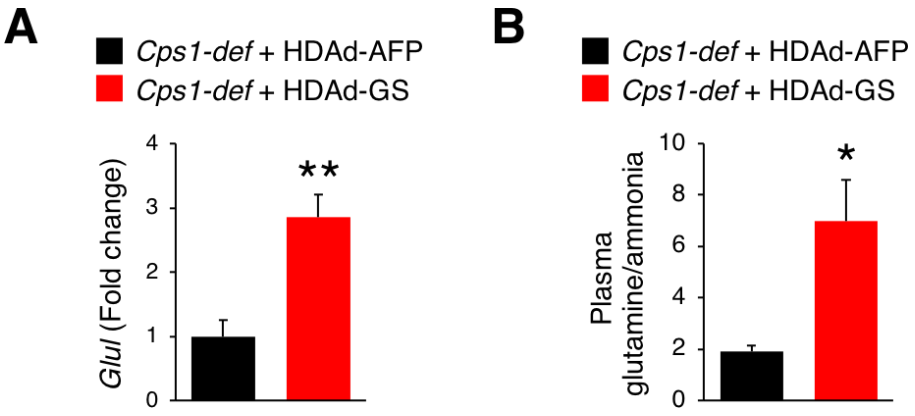

Figure 9. Expression of GS in livers of HDAd-GS- and HDAd-AFP-injected mice. **(A)** *Glul* mRNA levels of livers of *Cps1*-deficient (*Cps1*-def) mice injected with HDAd-GS or HDAd-AFP and harvested at day 28. **P < 0.01 (n = 5/group). **(B)** Plasma glutamine/ammonia ratio at day 28 in *Cps1*-def mice injected with HDAd-GS or HDAd-AFP. *P < 0.05 (n = 5/group). Abbreviations: AFP: α-fetoprotein; GS: glutamine synthetase; HDAd: helper-dependent adenoviral vector.

Cps1-deficient mice injected with HDAd-GS showed reduced serum ammonia at baseline and after i.p. challenge with ammonium chloride compared to *Cps1*-deficient mice injected with HDAd-AFP (**Fig. 10**). Notably, baseline plasma ammonia levels were reduced to wild-type levels in *Cps1*-deficient mice injected

with HDAd-GS. Reduction of ammonia levels was also detected at 20 and 60 minutes post-ammonia challenge although these levels were higher than wild-type mice.

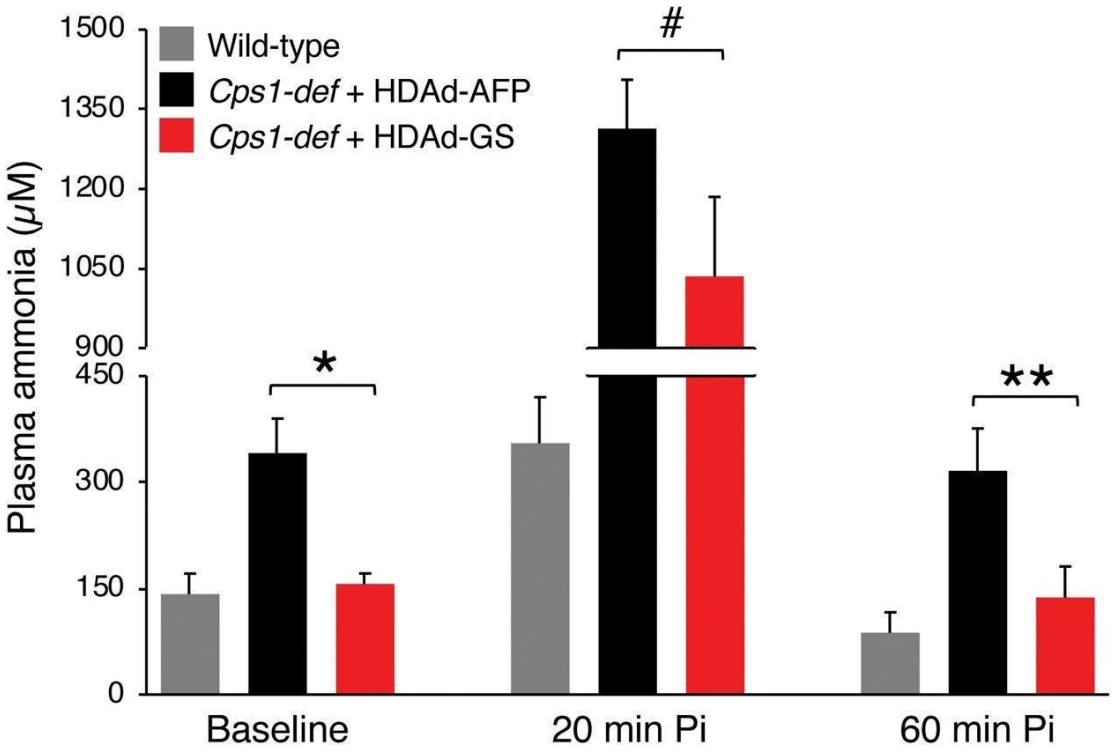

Figure 10. Liver-specific GS overexpression improved ammonia detoxification in *Cps1*-deficient mice. Plasma ammonia in *Cps1*-deficient (*Cps1-def*) mice injected with HDAd-GS (n = 9) or HDAd-AFP vector (n = 10) at baseline, 20 and 60 minutes after intraperitoneal injections of ammonium chloride (5 mmol/kg). #$P = 0.055$; *$P < 0.05$; **$P < 0.01$ (two-way ANOVA). Control ammonia-treated wild-type mice are also included (n = 5). Data represent averages ± SEM. Abbreviations: AFP, α-fetoprotein; GS, glutamine synthetase; HDAd, helper-dependent adenoviral vector; Pi, post injection.

Taken together, these results support the therapeutic potential of hepatic GS augmentation for treatment of acute hyperammonemia in an inherited ammonia detoxification disorder. Of note, these results were recently published in the journal *J Inherit Metab Dis* and I was included as co-author of this study [33].

AIM 2: To investigate pharmacologic modulation of O-GlcNAcylation for therapy of hyperammonemia

The first evidence that links O-GlcNAcylation to ammonia came from cultured rat astrocytes in which ammonia increases levels of O-GlcNAcylated proteins in a time and dose dependent manner [21]. To investigate the relationship between ammonia and O-GlcNAcylation, hepatic O-GlcNAcylation levels were analyzed under acute hyperammonemia condition (NH_4Cl:10 mmol/Kg i.p.) in C57BL/6 wild-type mice. An increase of hepatic O-GlcNAcylation occurred in response to ammonia challenge (**Fig. 11A,B).** Notably, UDP-GlcNAc levels increased in ammonia treated mice compared to the vehicle treated mice **(Fig. 11C)**. Next, I investigated the involvement of hepatic O-GlcNAcylation in ammonia detoxification.

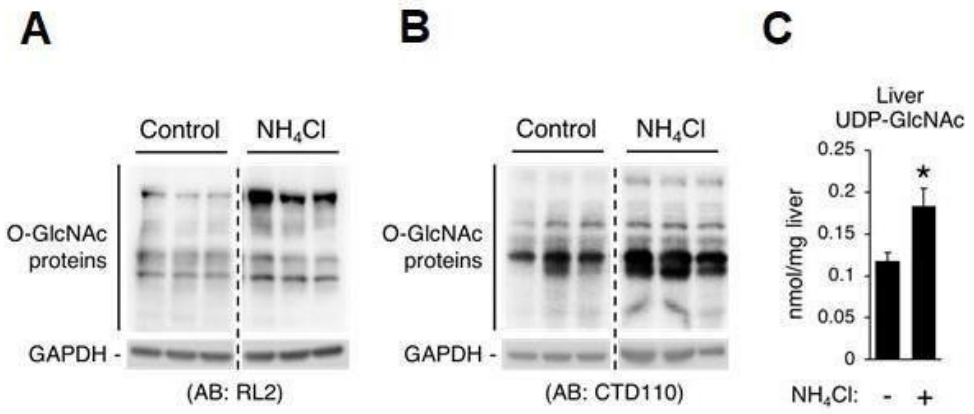

.

Figure 11. Acute hyperammonemia activates O-GlcNAcylation in liver. (**A-B**) Western blot of O-GlcNAcylated proteins of total lysates of liver of wild-type mice at baseline and 60 minutes after i.p. injection of ammonia load (NH_4Cl: 10 mmol/kg i.p. for 60 min). GAPDH was used as loading control. RL2 and CRD110 antibody were used to detec O-GlcNAcylated proteins. GAPDH was used as loading control. **C**) Hepatic UDP-GlcNAc levels harvested 60 minutes after injection of saline (control) or NH_4Cl. $P < 0.021565378$ (n=5/group).

To this end, C57BL/6 wild-type mice were injected with PUGNAc (7 mg/kg, i.p.) or Thiamet-G (40 mg/kg, i.p.) to increase liver O-GlcNAcylated proteins. Both PUGNAc and Thiamet-G are two

established and commercially available OGA inhibitors [34; 35]. Given its high selectivity for human OGA over other glycosidases and functionally related b-N-acetylglucosaminidases both *in vitro* and *in vivo*, Thiamet-G is accepted as a powerful tool for probing the functional role of O-GlcNAc [20; 36]. As expected, 48 h after treatments with either drug, O-GlcNAc protein levels were increased compared to vehicle-treated controls (**Fig. 12A**). Next, mice were treated with ammonia (NH_4Cl: 10 mmol/kg, i.p.) to induce acute hyperammonemia [37; 38]. Vehicle treated animals showed an increase of circulating ammonia at 0.5 h post-NH_4Cl challenge whereas lower serum ammonia levels were detected in mice treated with PUGNAc (**Fig. 12B**, orange bars) or Thiamet-G (**Fig. 12B**, blue bars).

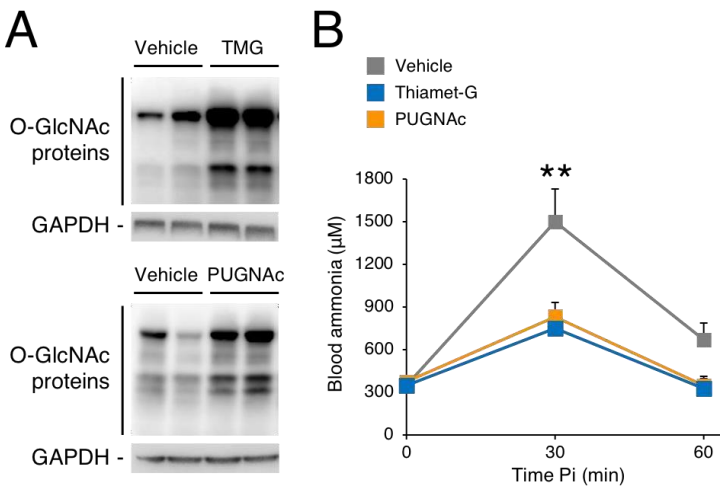

Figure 12. Increased O-GlcNAcylation reduces blood ammonia levels**.** (**A**) Western blot of hepatic O-GlcNac protein levels in hyperammonemic mice treated with OGA inhibitors: Thiamtet-G (40 mg/kg, i.p.) and PUGNAc (7 mg/kg, i.p.). GAPDH was used as loading control. (**B**) Serum ammonia levels at baseline and 60 min after i.p. of NH 4 Cl in mice pre-treated with PUGNAc or Thiamet-G compared to vehicle-treated controls. Data are expressed as means ± SEM. *p < 0.05; n ≥ 7. Abbreviations: TMG: Thiamet-G; Pi: post-injection.

Next, we evaluated ureagenesis by ^{15}N-NMR spectroscopy in PUGNAc and Thiamet G, as previously reported [37]. Interestingly, both PUGNAc and Thiamet-G mice showed an increased serum levels of ^{15}N-labeled urea (**Figure 13**), indicating increased ureagenesis. Liver content of glutamine instead was not affected by neither vehicle nor PUGNAc (**Fig. 14**). In summary, PUGNAc and Thiamet-G treatments improved ammonia detoxification capacity by increasing ureagenesis.

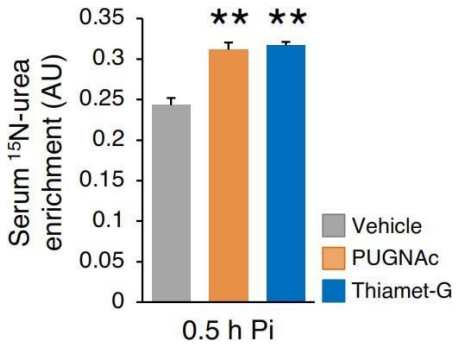

Figure 13. Hepatic O-GlcNAcylation increases ureagenesis. Serum levels of ^{15}N-labeled urea at 0.5 h after i.p. injection of $^{15}NH_4Cl$ in vehicle and OGA-inhibitors-treated mice. Data are expressed as means ± SEM. **P < 0.01; n ≥4/group. Abbreviations: pi: post-injection.

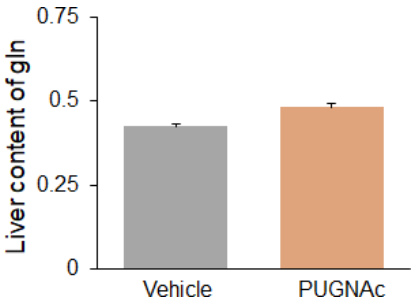

Figure 14. Hepatic O-GlcNAcylation does not affect glutamine levels. Glutamine levels in livers of mice treated with vehicle or PUGNAc. *P* < 0.088 (n ≥ 5/group). Abbreviation: Gln: glutamine.

Moreover, these results suggest that pharmacological enhancement of O-GlcNAcylation has potential for therapy of acute hyperammonemia. To confirm the role of OGA as a target for therapy of hyperammonemia, we performed *in vivo knock-down* of OGA that was confirmed by western blot (**Fig. 15**) .

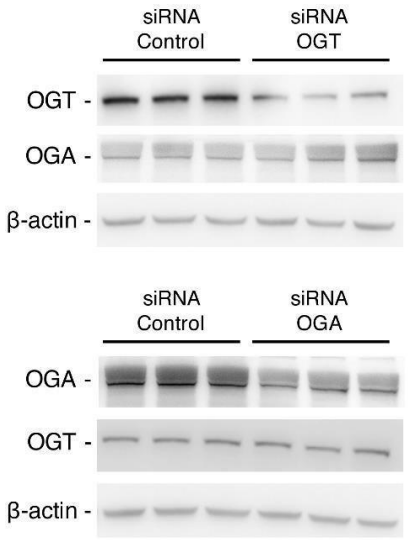

.

Figure 15. Western blot for OGT and OGA from livers of wild-type mice treated with specific siRNA against OGT and OGA (1 mg/kg, single injection, i.v.) harvested 6 days after siRNA administration. Control group received a commercial scrambled siRNA. β-actin was used as loading control. Abbreviations: ns: not significant.

As expected, an acute ammonia load increased hepatic O-GlcNAcylated protein levels compared to untreated animals but the increase in O-GlcNAcylation proteins was potentiated in mice with *knock-down* of OGA (**Fig. 16**).

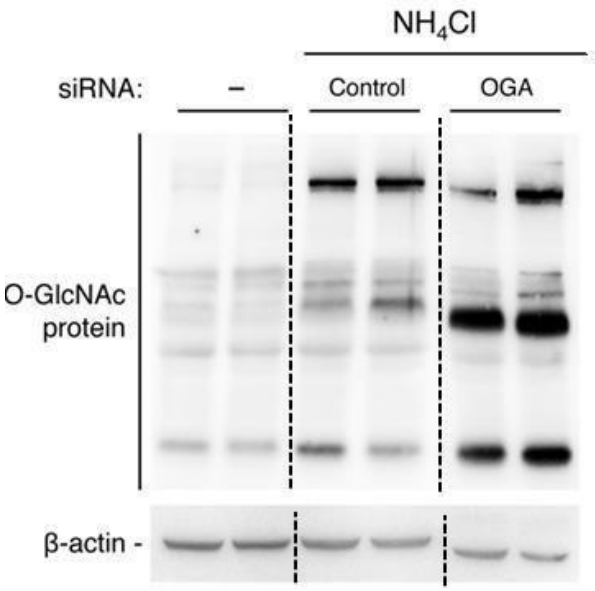

Figure 16. O-GlcNAc protein levels in livers from mice with OGA *knock-down* during acute hyperammonemia. β-actin was used as loading control.

Liver *knock-down* of OGA resulted in significantly lower ammonia levels compared to siRNA treated controls (**Fig. 17**).

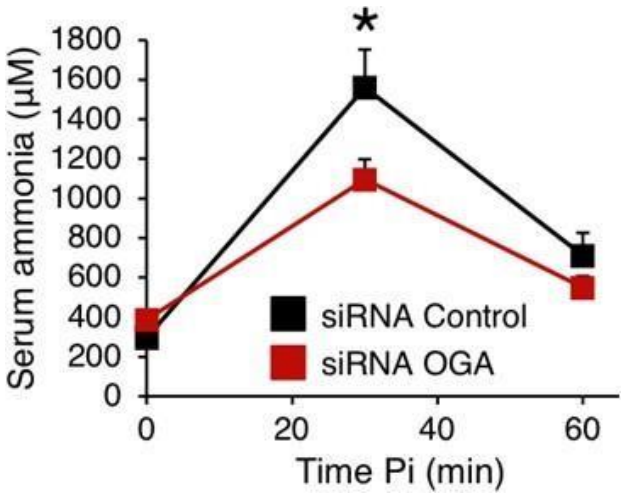

Figure 17. Serum ammonia at baseline, 30 and 60 min after i.p. injection of NH_4Cl in mice with OGA knock-down. *P < 0.05 (n ≥ 5/group). Abbreviations: pi: post-injection; ns: notsignificant.

The decreased ammonia was associated with enhanced ureagenesis in mice with siRNA-mediated hepatic knockdown of OGA (**Fig. 18**), as shown by by ^{15}N-NMR spectroscopy.

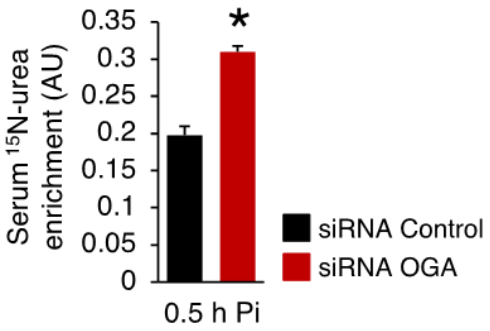

Figure 18. Serum levels of ^{15}N-labeled urea at 30 min after i.p. injection of $^{15}NH_4Cl$ in mice with OGA *knock-down* compared to controls. *P < 0.05 (n ≥ 5/group). Abbreviations: pi: post-injection.

Taken together, these results indicate that OGA is a drug target for treatment of hyperammonemia.

To investigate the mechanism underlying the protection against hyperammonemia induced by increased O-GlcNAcylation, I first evaluated gene expression of the urea cycle genes and other relevant genes encoding enzymes involved in ammonia detoxification by qPCR in mice treated with PUGNAc or Thiamet-G. As shown in **Fig. 19** expression of the evaluated genes was unaffected by OGA inhibition, neither their protein levels analyzed by western blot (**Fig. 20).**

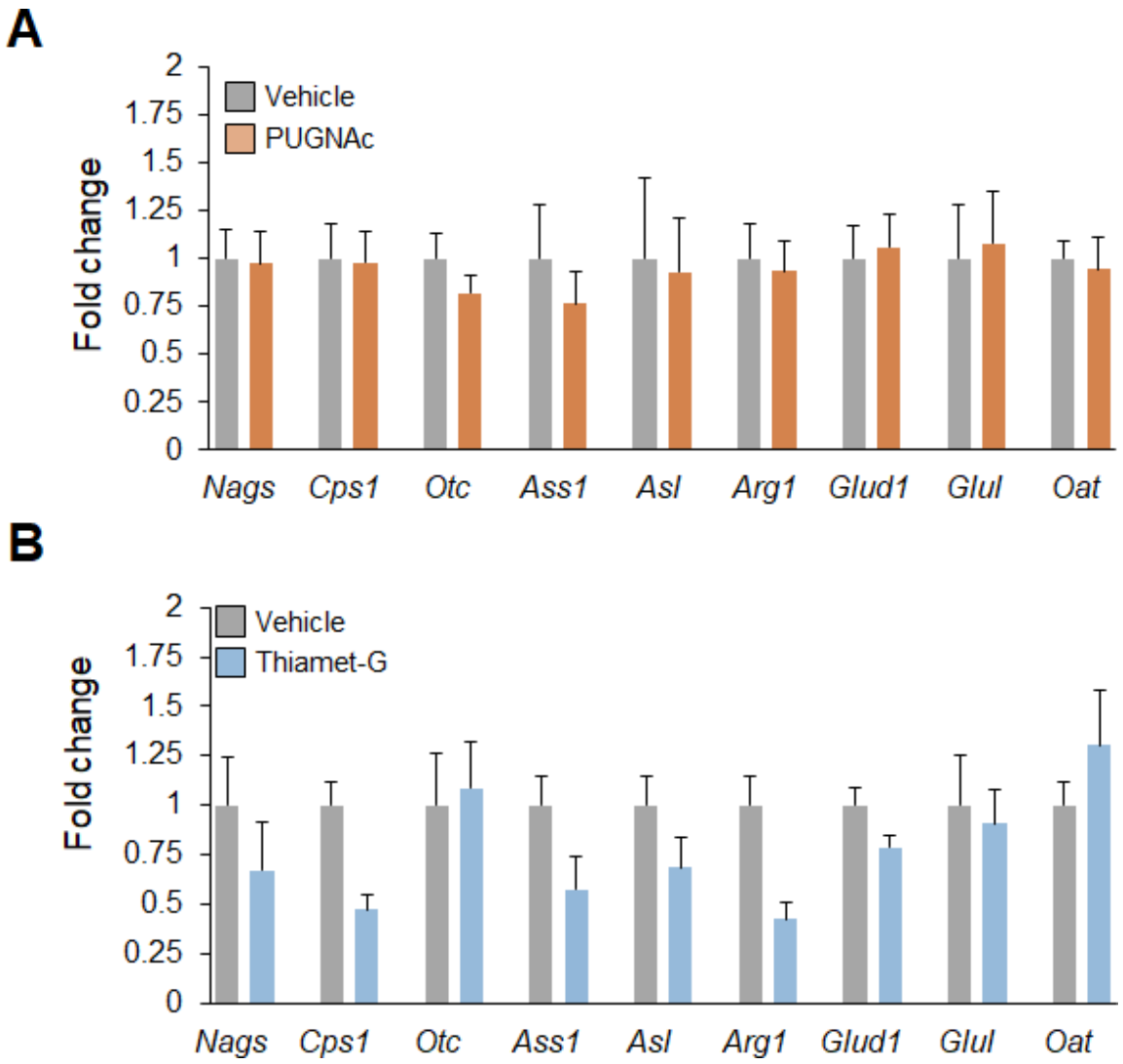

Figure 19. Gene expression of urea cycle enzymes were not affected by OGA pharmacologic inhibition. Relative expression levels of *Nags*, *Cps1*, *Otc*, *Ass1*, *Asl*, *Arg1*, *Glud*, *Glul*, and *Oat* mRNA in livers from mice treated with PUGNAc (7 mg/Kg i.p.) **(A)** and Thiamet-G (40 mg/Kg i.p.) **(B),** or vehicle. *$p < 0.05$ ($n \geq 4$/group).

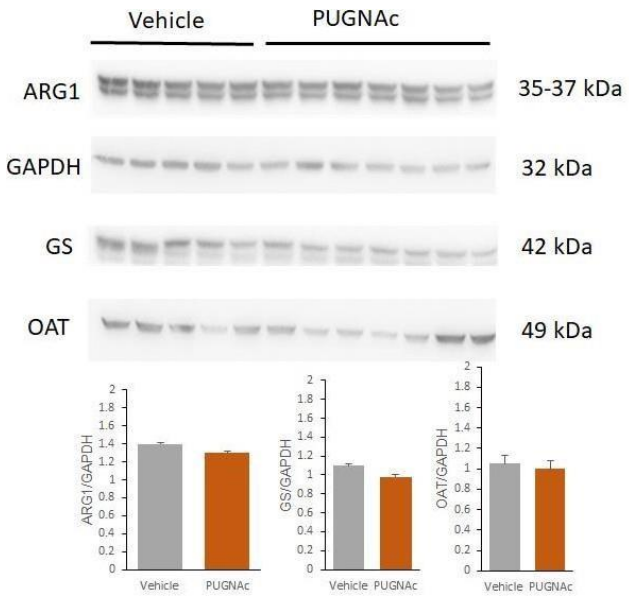
Vehicle
PUGNAc
ARG1
35-37 kDa
GAPDH
32 kDa
GS
42 kDa
OAT
49 kDa
ARG1/GAPDH
GS/GAPDH
OAT/GAPDH
Vehicle
PUGNAc

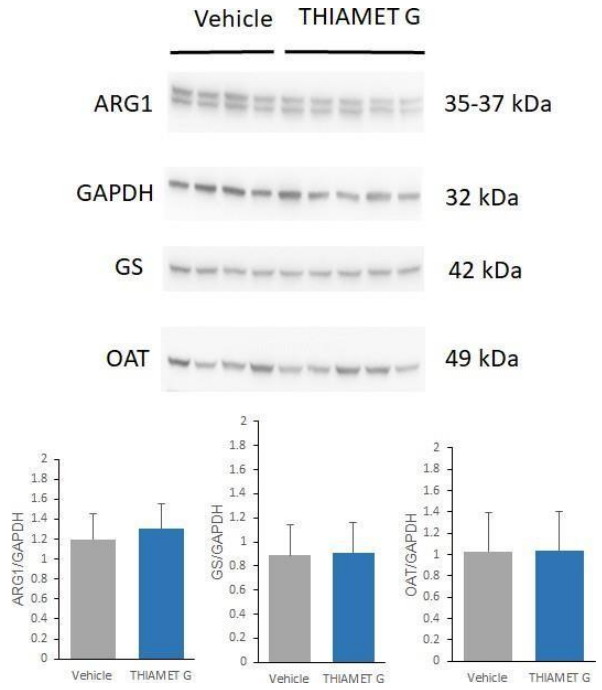
Vehicle
THIAMET G
ARG1
35-37 kDa
GAPDH
32 kDa
GS
42 kDa
OAT
49 kDa
ARG1/GAPDH
GS/GAPDH
OAT/GAPDH
Vehicle
THIAMET G

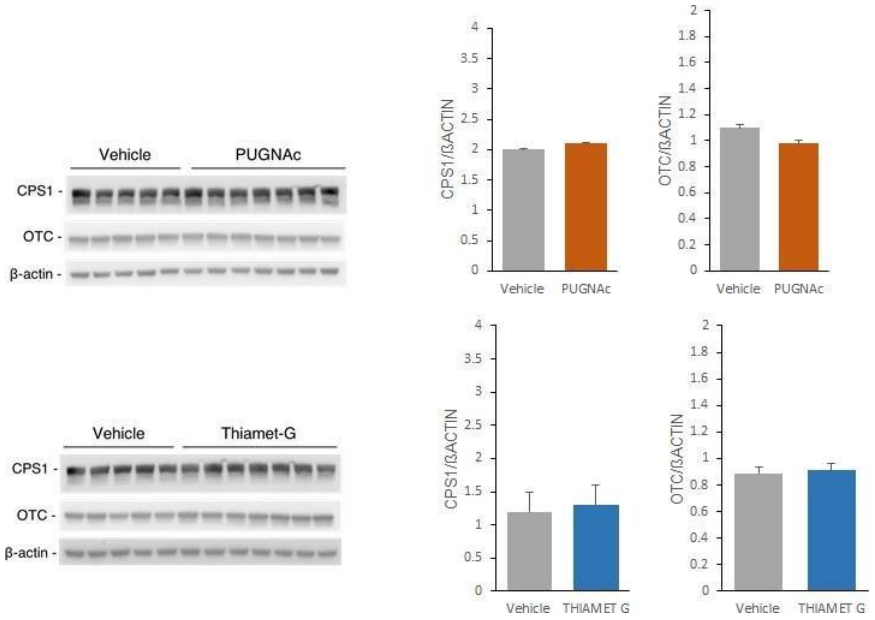

Figure 20. ARG1, GS, OAT, CPS1 and OTC protein expression was unaffected in livers of mice treated with OGA inhibitors. Western blot analysis of urea cycle proteins of total liver lysates of mice treated with PUGNAc (7 mg/Kg i.p.) and Thiamet-G (40 mg/Kg i.p.) or vehicle and their relative densiometric quantifications. β-actin and GAPDH were used as loading control.

Protein levels of CPS1, the initial and rate-limiting step of ureagenesis, were also unaffected by OGA inhibition. CPS1 is a mitochondrial enzyme (molecular weight 116 KDa) that synthesizes carbamoyl phosphate from bicarbonate and ammonia via three separate reactions: phosphorylation of hydrogen carbonate to carboxy-phosphate (using one ATP molecule); a nucleophilic attack of ammonia on carboxyphosphate yielding carbamate; and phosphorylation of carbamate forming carbamoyl phosphate (another ATP molecule consumed) (**Fig. 21)**. CPS1 requires the allosteric activator N-acetyl-L-glutamate. Interestingly, CPS1 has been previously found to be O-GlcNAcylated in three different domains: two of them are responsible for bicarbonate and carbamate phosphorylation; while the third O-GlcNAcylated domain is an integrating structural domain [39; 40; 41; 42]. Nevertheless, the functional consequence of CPS1 O-GlcNAcylation is unclear.

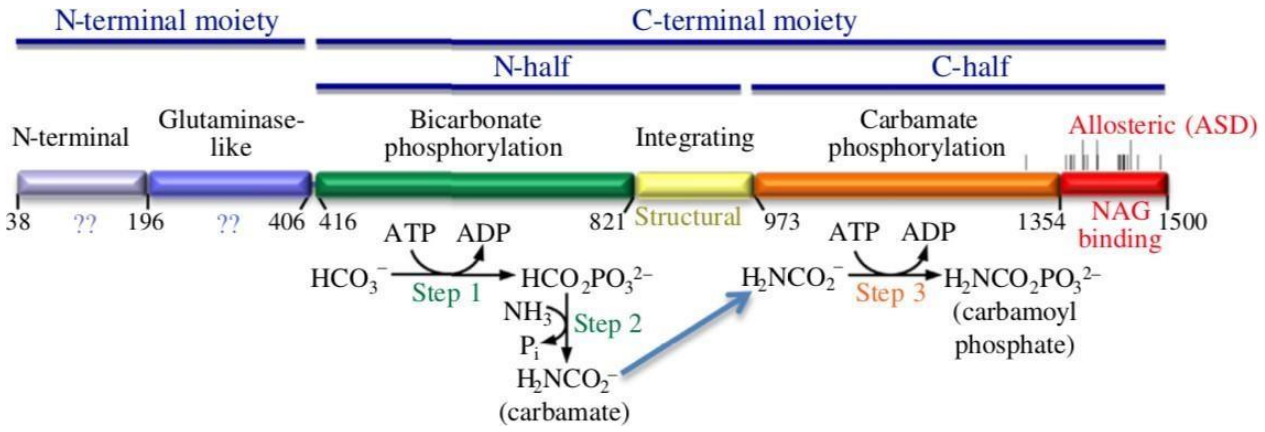

Figure 21. Scheme of the mature CPS1 protein with its two moieties (top). The middle bar indicates the two sequence-related halves of the large moiety. Domain composition with names and boundaries, given as residue numbers, is indicated in the lower bar. The three steps of the CPS1 reaction are shown below the corresponding domains where they occur. The blue arrow indicates carbamate migration between the phosphorylation active centers, a process contributed mainly by residues from both phosphorylation domains. Adapted from [43].

O-GlcNAcylation increases enzymatic activity of glucose-6-phosphate dehydrogenase (G6PD), the rate-limiting enzyme of the pentose phosphate pathway (PPP) [44] and I investigated whether CPS1 O-GlcNAcylation is increased by OGA inhibition both *in vitro* and *in vivo*. Hela cells were treated with PUGNAc or Thiamet-G to increase protein O-GlcNAcylation (**Fig. 22A**)**.** The same total cell lysates were immunoprecipitated with anti-CPS1 antibody or a control IgG. Immunoblotting assay showed that endogenous CPS1 was O-GlcNAcylated and O-GlcNAcylation increased upon OGA inhibition by PUGNAc or Thiamet-G compared to vehicle treated cells (**Fig. 22A)**. Murine CPS1 was also transfected in HEK293 cells and in HuH7 cells that were also treated with PUGNAc or Thiamet-G (**Fig. 22B-C**). Western blot of total lysates confirmed increased O-GlcNAcylation of CPS1 in PUGNAc or Thiamet-G treated HEK293 and HuH7 cells.

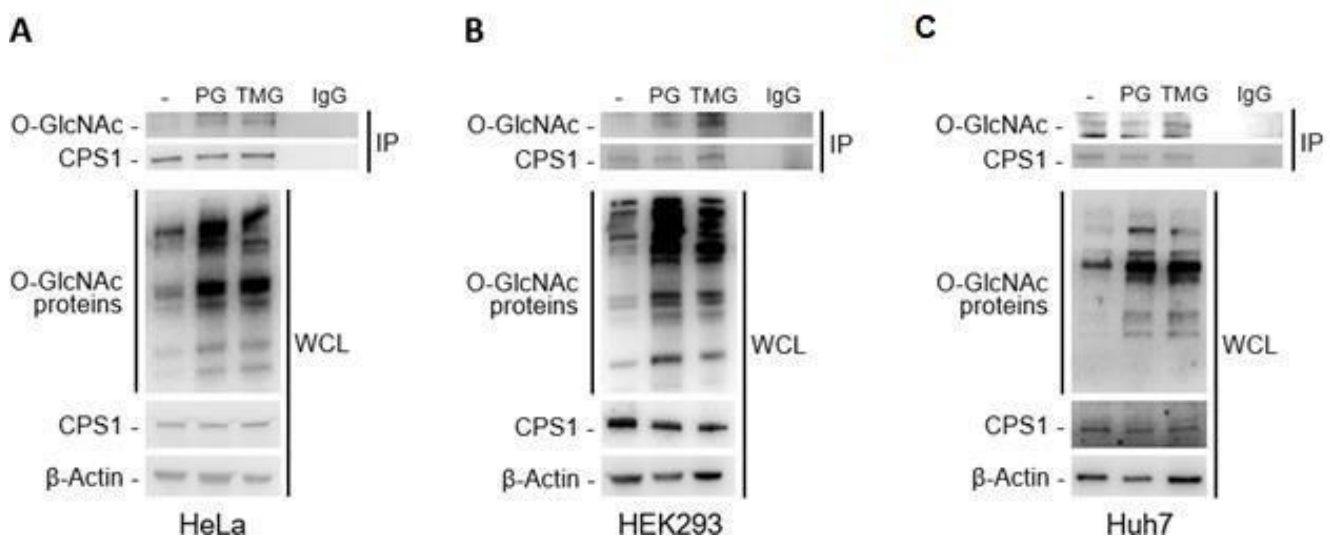

Figure 22. (**A**) HeLa cells were treated for 24 h with PUGNAc (100 µM) or Thiamet-G (10 µM). As expected, elevated O-GlcNAcylated proteins were detected in whole cell lysates (WCL-Input) whereas total amount of CPS1 was unaffected. Increased O-GlcNAcylation of CPS1 was in immunoprecipated CPS1. (**B**) HEK293 and (C) HuH7 cells were transfected with a plasmid encoding CPS1 for 48 hours and treated with PUGNAc (100 µM) or Thiamet-G (10 µM) for 24 hrs. Western blot of WCL and an IP are shown. Abbreviations: IP: immunoprecipitation; PG: PUGNAc; TMG: Thiamet-G; WCL: whole cell lysate.

Next, I investigated in vivo CPS1 O-GlcNAcylation in liver lysates of mice treated with OGA inhibitors by immunoprecipitation with an anti-CPS1antibody. CPS1 was confirmed to be O–GlcNAcylated that was increased by Thiamet-G (**Fig. 23).**

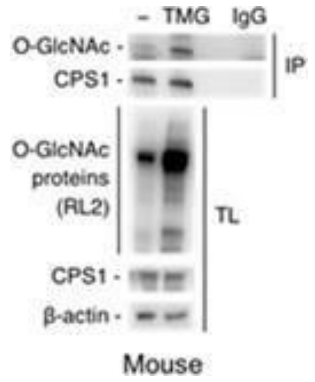

Figure 23. Wild-type mice were treated with Thiamet-G (40 mg/Kg) for two days i.p. or vehicle before proteins were isolated and subjected to direct immunoprecipitation with anti-CPS1 antibody. Western bot of input of total lysates is shown in the same panel. β-actin was used as loading control. IgG was used as negative control for IP experiments. Abbreviations: IP: immunoprecipitation; TL: total lysate; TMG: Thiamet-G.

Based on these results, I hypothesize that increased O-GlcNAcylation of CPS1 results in increased enzyme activity and ureagenesis. To confirm this hypothesis, kinetic studies to evaluate changes in substrate affinity (Km) and/or catalytic efficiency (kcat/Km) are currently ongoing in the laboratory of our collaborator, Johannes Haberle.

Discussion

Ammonia is a toxic compound daily generated in our organism that needs to be efficiently eliminated. The liver plays a major role in ammonia detoxification accomplished by the urea cycle in periportal hepatocytes and GS in the perivenous compartment. Notably, these two systems operate anatomically and functionally in sequence in the liver (metabolic zonation) [3]. The ureagenesis is a high-affinity system for ammonia detoxification in which CPS1 is the starter of the urea cycle and catalyzes the condensation of bicarbonate and ammonia to form carbamoylphosphate inside the mitochondrial matrix. The urea cycle is a sequence of six enzymatic and two transport steps needed to metabolize and excrete the nitrogen generated by the breakdown of amino acids in protein and other nitrogen-containing molecules. In contrast, the cytosolic GS is a cytosolic enzyme that catalyzes ATP-dependent production of glutamine from glutamate and ammonia. When the detoxification system fails or there is an increased production of ammonia, toxic ammonia accumulates within the body causing hyperammonemia [5]. Hyperammonemia can be classified into primary and secondary hyperammonemia and leads to encephalopathy which can manifest as cerebral edema, vomiting, blurred vision, asterixis, and seizures. It can also cause coma and irreversible brain damage if not treated early and thoroughly [5]. Treatments against hyperammonemia are insufficient and more effective therapy are needed. The aim of the present thesis work is to study new and effective therapies for the treatment of hyperammonemia investigating both hepatic GS augmentation and modulation of O- GlcNAcylation. For GS augmentation, we used a helper dependent adenoviral vector to deliver the murine GS to hepatocytes. Notably, increased levels of hepatic GS provided an amelioration of

detoxification, protecting wild-type mice against acute hyperammonemia. Moreover, the same vector was used also to deliver GS to *Cps1* deficient mice resulting in reduction of plasma ammonia levels. In summary, in two different models of hyperammonemia (primary and secondary) we showed that GS augmentation is effective for therapy of hyperammonemia. In addition, treatments aiming at increasing GS activity can be combined with available treatments such as low protein diet, ammonia scavengers, or the recently described activation of hepatic autophagy [37] to obtain more effective control of blood ammonia levels. Interestingly, improved ammonia control can be obtained by supplementation with glutamate (or its precursors) or phenylacetate to enhance ammonia removal by increased synthesis and clearance of glutamine, respectively [45]. Hepatic GS upregulation might also be achieved by systemic mRNA delivery, a therapeutic strategy that has been successfully used for correction on an inborn error of metabolism [46]. Moreover, GS augmentation therapy might be achieved by uploading of GS onto lipid- or polymeric-based nanoparticles [47] for systemic delivery or with membrane derived from natural cells such as erythrocytes or white blood cells [48]. In addition, ammonia detoxification may be further improved by vesicles uploaded with recombinant GS enzyme through liposome-supported peritoneal dialysis [49]. Small molecule drugs upregulating hepatic GS expression are another attractive approach. Interestingly, glucocorticoids are known to positively regulate expression of GS at the transcriptional level in multiple tissues [50]. Dexamethasone was indeed found to be effective in mice at increasing ammonia detoxification [48]. However, overexpression of GS in astrocytes is likely to be detrimental because it could lower the threshold of brain toxicity since cerebral edema depends on glutamine synthesis in astrocytes [51]. Hence, treatments with low glucocorticoid doses or other drugs upregulating GS in livers but not in astrocytes are desirable. Current guidelines for management of patients with suspected or confirmed diagnosis of urea cycle disorders recommend avoidance of steroids because they induce protein catabolism and can trigger hyperammonemia [52]. This recommendation is based on anecdotal experience in patients with acute decompensation following steroid treatments [53]. The results of our study suggest that GS upregulation is protective against hyperammonemia although the increased

GS expression in astrocytes is likely to be detrimental.

Furthermore, I investigated the correlation between ammonia and O-GlcNAcylation. O-GlcNAcylation (O-GlcNAc) is a post-translational modification (PTM) consisting of non-canonical glycosylation with the attachment of O-linked N-acetylglucosamine (O-GlcNAc) to serine and threonine residues of proteins [22]. Reversible protein O-GlcNAcylation was found to be induced by ammonia treatment in rat astrocytes suggesting that O-GlcNAcylation is involved in the pathophysiology of hepatic encephalopathy [21]. Hence, the role of hepatic O-GlcNAcylation in ammonia detoxification was investigated. Towards this goal, I examined the efficacy of pharmacologic modulation of O-GlcNAcylation on improving ammonia detoxification capacity. In vivo modulation of O-GlcNAcylation through OGA inhibitors and OGA knockdown approaches improved ammonia detoxification. Therefore, OGA is a promising therapeutic target for therapy of acute hyperammonemia. Moreover, I investigated the mechanism underlying the protection against hyperammonemia induced by increased O-GlcNAcylation. Neither gene nor protein expression levels of urea cycle enzymes were increased by OGA inhibition, suggesting that hepatic O-GlcNAcylation regulates ammonia clearance capacity by affecting enzymatic activity of the urea cycle. In particular, I focused my attention on carbamoyl phosphate synthetase I (CPS1), the initial and rate-limiting step of ureagenesis. This enzyme has been previously found to be O- GlcNAcylated in three different domains [39; 40; 41; 42] with unknown functional consequences. I confirmed that CPS1 is O-GlcNAcylated and that its level of O-GlcNAcylation is increased upon OGA inhibition by two independent methods. Based on these results, I hypothesized that increased O-GlcNAcylation of CPS1 results in increased enzyme activity and ureagenesis. However, further studies are needed to show whether CPS1 with increased O- GlcNAcylation has higher catalytic activity.

Materials and Methods

Mouse studies. Male wild-type (WT) 6-week-old C57BL/6 (Charles River Laboratories, Calco, Italy) and adult female transgenic $Cps1^{tm1c/tm1c}$mice [32] were randomly assigned to treatment groups. Investigators were not blinded to allocation during experiments and outcome assessment. All intravenous (i.v.) injections were performed by retro-orbital injections under isoflurane anesthesia. Vectors were prepared in sterile pharmaceutical-grade saline. Male and female mice were equally represented throughout the study. WT and $Cps1^{tm1c/tm1c}$mice were injected with a dose of 1×10^{13} viral particles (vp)/kg of helper-dependent adenoviral (HDAd)-GS or HDAd-alpha-fetoprotein (AFP) (α-fetoprotein) as a control [32]. The ammonium intraperitoneal (i.p.) challenge in WT mice was performed at 4 weeks post vector injection. Mice were overnight fasted before i.p. injections of 10 mmol/kg of ammonium chloride (Merck, Darmstadt, Germany) dissolved in water [37]. Three days after the injections of HDAd expressing either AFP or GS, $Cps1^{tm1c/tm1c}$mice were injected with 1.5×10^{10}genome copies (gc)/mouse of AAV8 vector expressing Cre recombinase under the control of the thyroxine binding globulin promoter (liver-specific) [33]. $Cps1^{tm1c/tm1c}$mice were weighed daily and monitored for any signs of poor health. In $Cps1^{tm1c/tm1c}$mice, the i.p. ammonia challenge was also performed 4 weeks after the injections of the HDAd vectors but with a lower dose of i.p. 5 mmol/kg ammonium chloride and without prior fasting. Male wild-type 6-week-old C57BL/6 (Charles River Laboratories, Calco, Italy) were injected i.p. with Thiamet-G (Sigma-Aldrich; 40 mg/kg, for two days before i.p. injections of 10 mmol/kg of ammonium chloride) and PUGNAc (Sigma-Aldrich; 7 mg/kg, for two days before the ammonia i.p. injections). Both drugs were dissolved in PBS. Male WT 6-week-old C57BL/6 (Charles River Laboratories, Calco, Italy) were depleted of OGT or OGA in the liver by using the Invivofectamine $^{3.0}$ reagent system (Cat#: IVF3001; ThermoFisher, Milan S.R.L.). The commercially available siRNA duplex solution was prepared and diluted according to the manufacturer's instructions. Preparation of the final injection solution was performed following the established Thermofisher protocol. Briefly, the same day of administration corresponding pre-

designed siRNA (ThermoFisher) were mixed with the complexation buffer and then the Invivofectamine® 3.0 reagent. The solution was vortexed, incubated at 50°C for 30 min and finally diluted in sterile PBS. Intravenous (i.v.) administration was performed by retro-orbital injection of 200 µl of solution at a final concentration of 1 mg/kg. No adverse side effects were observed after injection. Control mice received the Silencer™ Select Negative Control No.1 siRNA (Cat#: 4390843, ThermoFisher, Milan S.R.L.). To induce hepatic *knock-down* of OGT, mice received a mix of pre-designed siRNA to deplete murine OGT (ID: #173150 and #173151; Cat#AM16708, ThermoFisher, Milan S.R.L.). Similarly, to induce *knock-down* of OGA in liver, mice received a mix of pre-designed siRNA against mouse OGA (MGEA5 gene) (ID: #167691 and #167693; Cat#: AM16708, ThermoFisher, Milan S.R.L). The knockdown was left for 6 days and then animals were subjected to an acute ammonia load. Livers were harvested and specific *knock-down* efficacy was evaluated by western blot analysis. Blood samples were collected by retro-orbital bleedings at the indicated time points. Mice were sacrificed by cervical dislocation or isoflurane overdose. Serum or plasma and liver samples were harvested and stored at -80° C until analyses. Mouse procedures were performed in accordance with regulations and were authorized by both the Italian Ministry of Health and the Institutional Animal Care and Use Committee (IACUC) of David Geffen School of Medicine at UCLA, Los Angeles, United States.

Helper-dependent adenoviral (HDAd) vectors. HDAd-GS and HDAd-AFP vectors both bear a liver-specific expression cassette driving the expression of either mouse GS or baboon alpha-fetoprotein (AFP), respectively [28]. HDAd vectors were produced as previously reported [54] in 116 cells regularly tested and found negative for *Mycoplasma* by quantitative real time polymerase chain reaction PCR. Mouse GS cDNA and mouse Cps1 cDNA were synthesized by Life Technologies (Carlsbad, CA) [32].

Cell culture and transfection. HeLa and Hek293 cells were cultured in Dulbecco's modified Eagle's medium and 10% fetal bovine serum and 1% penicillin/streptomycin at 37°C in 5% CO_2. Cells were transfected with the PEPCK-WL-CPS1 plasmid using LipoD293™ DNA transfection reagent (Cat# Sl 100668; Ver.II, Tebu Bio S.R.L, Milan) according to manufacturer's instructions. After 24 h of transfection, Thiamet-G (10 µM) or PUGNAc (100 µM) were added to the medium; both were dissolved in PBS. PEPCK-WL-CPS1 plasmid bears the expression cassette including the liver-specific promoter of phosphoenolpyruvate carboxykinase (PEPCK) and other regulatory elements like the woodchuck hepatitis virus post regulatory element (WPRE), the Locus Control Region (LCR) from the apoE locus, the bovine growth hormone polyadenylation signal as described elsewhere [27; 28].

Immunoprecipitation (IP). For immunoprecipitation, cells and liver samples were lysed in cold RIPA lysis buffer (50 mM Tris-HCl [pH 7.4], 150 mM NaCl, 1% Triton X-100, 1 mM EDTA, 0.1% SDS and 1mM Thiamet G) in the presence of protease inhibitors (Sigma-Aldrich). The lysates were incubated on ice for 20 minutes with gentle swirling and centrifuged at 13 200 rpm for 10 minutes to pellet nuclei and cell debris. The supernatants were collected and subjected to protein quantification using the Bradford Reagent (Bio-Rad, Hercules, California, USA). 300 µg of each lysate was then incubated with 3 µl of antibody anti-CPS1 antibody (Cat# ab45956;Abcam, Cambridge, UK) (100µg proteins:1 µl antibody ratio) or anti rabbit IgG isotope as negative control (Cat# 31235 Thermo Fisher Scientific-0.4 ug/ul) and subjected to immunoprecipitation at 4°C overnight. The day after each immunoprecipitate was incubated with magnetic beads Dynabeads™ Protein G (Cat# 1004 D Thermo Fisher Scientific) for 2 hours at 4 °C. Immunoprecipitaton binded with the beads Dynabeads™ Protein G is separated from flow through with DynaMag™ magnet (Cat# 12321D Thermo Fisher Scientific) that is optimized for efficient magnetic separation of Dynabeads® due to the unique magnetic properties of Dynabeads, according to the manifacture's protocol. Then

immunoprecipitation-Dynabeads™ Protein G complex was washed thrice with PBS containing 0.02% Tween-20 before precipitated proteins were eluted through DynaMag™ magnet using 2× Laemmli sample buffer (1v/v). Finally, IP samples were put at 100 ° C for 5 minutes and analyzed by SDS–PAGE in a 7.5% gel.

Analyses of serum and plasma samples. Serum or plasma ammonia levels were measured by an ammonia colorimetric assay kit (Cat# K370-100; BioVision Incorporated, Milpitas, California, USA or Cat# ab83360; Abcam, Cambridge,UK), respectively. Serum or plasma glutamine concentrations were measured by a colorimetric assay kit (Cat#K556-100; BioVision Incorporated, Milpitas, California, USA). Serum urea content was determined by an assay kit based on Jung's method (Cat# K376-100; BioVision Incor-porated, Milpitas, California, USA). For blood urea nitrogen (BUN), 10μL of plasma per sample were pipetted into cups and placed into a Vet Excel Clinical Chemistry Analyzer (Alfa Wassermann Diagnostic Technologies, West Caldwell, New Jersey, USA). Calculation of urea nitrogen concentration was performed automatically by the clinical chemistry system. Hepatic ATP determination was performed by a fluorometric assay kit according to the manufacturer'sinstructions (Cat# K354-100; BioVision Incorporated, Mil-pitas, California, USA). Liver lysates were homogenized in the corresponding hydrolysis buffer using a Tissue Lyser LT (Qiagen, Venlo, Netherlands). Hepatic ATP levels were normalized for protein concentrations determined by Bradford Reagent (Bio-Rad, Hercules, California, USA).

UDP-GlcNAc analysis. Hepatic level of UDP-GlcNAc was determined by hydrophilic interaction liquid chromatography (HILIC) at the Academic Medical Center (Amsterdam, the Netherlands).

Western blot analysis. Liver specimens and cell samples were homogenized in RIPA buffer in the presence of complete protease inhibitor cocktail (Sigma-Aldrich,St. Louis, Missouri, USA), incubated for 20 minutes at 4° C and centrifuged at 13 200 rpm for 10 minutes. Pellets were discarded

and supernatants were used for western blots. Total protein concentration in cellular extracts was measured using the Bradford Reagent (Bio-Rad, Hercules, California, USA). Protein extracts were separated by sodium dodecyl sulphate-polyacrylamide gel electrophoresis (SDS-PAGE) and transferred onto hydrophobic polyvinylidene fluoride membranes (Immobilon-P PVDF Membrane, Merck). Blots were blocked with trisbuffered saline (TBS)-Tween-20 containing 5% nonfat milk for 1 hour at room temperature followed by incubation with primary antibody overnight at 4°C. Primary antibodies were: rabbit anti-Glutamine Synthetase (GS) (Cat# b16802; Abcam, Cambridge, UK), mouse anti-O-GlcNAcylation RL2 (Cat # Ab2739; Abcam, Cambridge, UK) and mouse anti-O-GlcNAcylation CTD110.6 (Cat # 9875; Cell Signaling), mouse anti- Glyceraldehyde 3-phosphate dehydrogenase (GAPDH) (Cat# sc-32233; Santa Cruz Biotechnology), rabbit anti-Ornithine Amino Transferase (OAT) (Cat# ab137679; Abcam, Cambridge, UK), mouse anti-Beta actin (ACTB) (Cat# NB600-501;Novus Biological), rabbit anti-Arginase(ARG1) (Cat# ab91279;Abcam, Cambridge, UK), rabbit anti-Carbamoyl phosphate synthetase 1 (CPS1) (Cat# ab45956;Abcam, Cambridge, UK) and rabbit anti-Ornithine Carbamoyl Transferase(OTC) (Cat# NBP1-31582, Novusbio), anti rabbit anti-p115 [54], mouse anti-O-GlcNAcTransferase (OGT) (Cat# ab184198;Abcam, Cambridge). Proteins of interest were detected with horseradish peroxidase-conjugated goat anti-rabbit or anti-mouse IgG antibody (GE Healthcare, Chicago, Illinois, USA). Peroxidase substrate was provided by enhanced chemiluminescence (ECL) Western Blotting Substrate kit (Pierce, Waltham, Massachusetts, USA). Densitometric analyses of the western blotting bands were performed using Image J Software (National Institutes of Health, Bethesda, Maryland, USA).

Immunofluorescence. Immunofluorescence was performed as previously described [32]. Liver sections were fixed in 10% neutral buffered formalin, stored in 70% ethanol and embedded in paraffin blocks followed by cutting the sections at 4-μm thickness. Sections were then deparaffinized in xylene and rehydrated in serial ethanol washes. Antigen retrieval was performed in 10-mM sodium citrate

buffer pH 6.0, after which the sections were permeabilized in 0.1% Triton X-100 and blocked with 10% normal goatserum. Slides were incubated with anti-carbamoyl phosphatesynthetase 1 (CPS1) antibody (Cat# ab45956; Abcam, Cam-bridge, UK) and anti-GLUL antibody (Cat# ab64613; Abcam, Cambridge, UK), both at 1μg/mL in the blocking buffer overnight at 4°C. Secondary antibody staining was performed at room temperature for 1 hour using Alexa Fluor594 goat anti-rabbit (A- 11012; Invitrogen, San Diego, Cali-fornia, USA) and Alexa Fluor 488 goat antimouse (A-11001; Invitrogen, San Diego, California, USA) antibodies. Cell nuclei were counterstained with 4',6- diamidino-2-phe-nylindole (DAPI) using VECTASHIELD Antifade Mount-ing Medium. Visualization of the stained sections was performed using Olympus IX71 Fluorescence Microscope.

RNA extraction and real-time PCR

RNA extraction and real-time PCR were performed as previously descrived [33]. Liver pieces were homogenized, and RNA was extracted by column purification (Cat# 11828665001; Roche Mannheim, Germany). Purified RNA was used to generate cDNA (Cat#04379012001; Roche Mannheim, Germany) for qPCR with BioRad SYBR Green (Cat# 1725270; Bio-Rad, Hercules, California, USA), and IQ2 iCycler. β-actin gene was used as endogenous control. Fold changes were calculated using the delta-delta-Ct (DDCt) method. *Cps1* primers were: forward CACCAATTTCCAGGTGACCA; reverse TACTGCTT-TAGGCGGCCTTT; *Glul* primers were: forward CCACTT-GAACAAAGGCATCA; reverse GTCCTTCTCCGGTACCATCA; *Actb* primers were: forward CTAAGGCCAACCGT-GAAAAG; reverse ACCAGAGGCATACAGGGACA.

Total RNA from livers was extracted using the RNeasy mini kit (Qiagen). RNA was retrotranscribed using the High-Capacity cDNA Reverse Transcription Kit (Applied Biosystems). Quantitative PCRs were set up using SYBR Green Master Mix and run in duplicate on a Light Cycler 480 system (Roche). The running program was as follows: preheating, 5 minutes at 95 °C: 40 cycles of 15 seconds at 95 °C, 15 seconds at 60 °C, and 25 seconds at 72 °C. Mouse β2-microglobulin (B2m) was used as

housekeeping genes. Data were analyzed using LightCycler 480 software, version 1.5 (Roche). Primers used are reported previously [55] and were:

Arg1: forward CATTGGCTTGCGAGACGTAGAC; reverse GCTGAAGGTCTCTTCCATCACC

Asl; forward CTGCAGGGAAGCTACACACA; reverse CGGAGAGTTTTGAGCAGGTC

Ass1: forward AACATTGGCCAGAAGGAAGA; reverse CCACAAATTCCTTGCTCACA

Cps1: forward CATCCGCCTGCTAGTTAAGC; reverse CCCAGCAATCAAAAGTCCAT

Gls2: forward CAGGAGCGTATCCCTATCCA; reverse CTGCATCTTGCTCATGCAGT

GluD1: forward GTCAGCGATCCAGGACATCT; reverse CTATGGAGCTGGCCAAGAAG

Glul: forward CCACTTGAACAAAGGCATCA; reverse GTCCTTCTCCGGTACCATCA

Nags: forward ACCTGTTGCAGTGGTGTCTG; reverse GTCACCTCCAGCGAGTCAAG

Oat: forward TGTAGCCCTGGAGAGAGGA; reverse CTTGGCTGACAGCACCATAA

Otc: forward GGATAGGGGATGGGAACAAT; reverse TCTGGCTCATAACCCTTTGG

Determination of ^{15}N-labeled urea by nuclear magnetic resonance spectroscopy (NMR). C57BL/6 wild-type mice were injected i.p. with Thiamet-G or PUGNAc or OGT and OGA siRNA or vehicle prior to the i.p. injection of 10 mmol/kg of ^{15}N-labeled ammonium chloride (98% enriched in 15N, Sigma). Blood samples were collected by retro-orbital bleedings at 0, 30 and 60 min post-injection. The amount of ^{15}N-labeled urea in sera was evaluated by comparison to ^{15}N-leucine signal added to all samples as an internal reference as previously described [37]. Biological ^{15}N-labeled urea in each sample was quantified from the observed ^{15}N peak intensities (in integrated areas) compared to the internal standard. One-dimensional (1D) ^{15}N spectra were recorded at 44.55 MHz on a Bruker AVANCE™III HD-400 spectrometer, equipped with a BBO BB-H&F-D CryoProbe™ Prodigy fitted with a gradient along the Z-axis, at a probe temperature of 27°C (300 K). The pulse Ineptrd sequence

(INEPT for non-selective polarization transfer with decoupling during acquisition) was used with the following parameters: d1 = 5 s, J = 9 0Hz, ns = 15000 and acquisition time of 0.809 s. The leucine signal was assumed to resonate at 18.00 ppm, and therefore the urea signal resonated at 55.80 ppm.

Metabolite profiling of liver tissue by ^{1}H-NMR. Tissues were mechanically disrupted to extract the metabolites of interest (lipids, carbohydrates, amino acids, and other small metabolites) while leaving other compounds (DNA, RNA, and proteins) in the tissue pellet. Homogenization of 200 mg of frozen tissue samples was carried out in 8 ml/g of wet tissue made of methanol and 1.70 ml/g per wet tissue of water (all solvents were cold) with UltraTurrax for 2 min on ice. 4 ml/g wet tissue of chloroform were added and the homogenate was gently stirred and mixed on ice for 10 min (the solution must be mono-phasic). Then, additional 4 ml/g wet tissue of chloroform and 4 ml/g wet tissue of water were added and the final mixture was well shaken and centrifuged at 12,000 g for 15 min at 4°C. This procedure separates three phases: water/methanol on the top (aqueous phase with the polar metabolites), denatured proteins and cellular debris in the middle, and chloroform at the bottom (lipid phase with lipophilic compounds). The upper and the lower layers were transferred into glass vials, the solvents removed under a stream of dry nitrogen, and stored at -80°C until the analyses [37].

NMR data processing and statistical analysis. The spectral 0.50–9.40 ppm region of the high-resolution 1H-NMR spectra was automatically data reduced to integrated regions (buckets) of 0.04-ppm each using the AMIX 3.6 package (Bruker Biospin, Germany). The residual water resonance region (4.72–5.10 ppm) was excluded, and the integrated region was normalized to the total spectrum area. To differentiate liver tissues through NMR spectra, we carried out a multivariate statistical data analysis using projection methods. The integrated data reduced format of the spectra was imported into SIMCA-P+ 15 package (Umetrics, Umea, Sweden) [37].

Statistical analyses. Data are expressed as means ±SEM. A two-tailed unpaired Student's t-test was performed when comparing two groups of mice. One-way ANOVA and Tukey's post-hoc tests were

performed when comparing more than two groups relative to a single factor. Two-way ANOVA and Tukey's post-hoc tests or Sidak's multiple tests were performed when comparing two groups relative to two factors. No statistical methods were used to predetermine the sample size. A *P*-value < 0.05 was considered statistically significant [33].

References

1. Adeva M, et al., A*mmonium metabolism in humans.* Metabolism, 2012. 6 1(11):1495-511.
2. Coomes MW, *Amino acid metabolism*. IN: Devlin TM, editor. Textbook of biochemistry with clinical correlations. Hoboken, NJ: Wiley-Liss; 2006. P.743-82
3. Haussinger D, *Nitrogen metabolism in liver: structural and functional organization and physiological relevance*. Biochem J. 1990. 267: 281-290.
4. Spodenkiewicz M, et al., *Minireview on Glutamine Synthetase Deficiency, an Ultra-Rare Inborn Error of Amino Acid Biosynthesis.* Biology (Basel), 2016. 19;5(4).
5. Haberle J, *Clinical and biochemical aspects of primary and secondary hyperammonemic disorders.* Arch Biochem Biophys. 2013. 5 36(2):101-8.
6. Diez-Fernandez C, et al., *Understanding carbamoyl phosphate synthetase (CPS1) deficiency by using the recombinantly purified human enzyme: effects of CPS1 mutations that concentrate in a central domain of unknown function.* Mol Genet Metab. 2014. 112: 123-132.
7. Stewart PM, et al., *Failure of the normal ureagenic response to amino acids in organic acid-loaded rats. Proposed mechanism for the hyperammonemia of propionic and methylmalonic acidemia.* J Clin Invest. 1980. 66: 484-492.
8. Aires CC, et al., *New insights on the mechanisms of valproate-induced hyperammonemia: inhibition of hepatic N-acetylglutamate synthase activity by valproyl-CoA.* J Hepatol. 2011. 55: 426-434.
9. Haberle J, et al., *Congenital glutamine deficiency with glutamine synthetase mutations*. N Engl J Med. 2005. 353: 1926-1933.
10. Haberle J, et al., *Natural course of glutamine synthetase deficiency in a 3 year old patient*. Mol. Genet. Metab. 2011. 103(1):89-91.

11. Gebhardt R, et al., *Changes in distribution and activity of glutamine synthetase in carbon tetrachloride-induced cirrhosis in the rat: potential role in hyperammonemia.* Hepatology, *1994. 20: 684-691.*

12. Qvartskhava N, et al., *Hyperammonemia in gene-targeted mice lacking functional hepatic glutamine synthetase*. Proc Natl Acad Sci. 2015. 112: 5521-5526.

13. Jover-Cobos M, et al., *Ornithine phenylacetate targets alterations in the expression and activity of glutamine synthase and glutaminase to reduce ammonia levels in bile duct ligated rats*. J Hepatol. *2014.* 60: 545-553.

14. Matoori S, et al., *Recent advances in the treatment of hyperammonemia*. Adv Drug Deliv Rev. 2015. 90: 55-68.

15. Torres-Vega MA, et al., *Delivery of glutamine synthetase gene by baculovirus vectors: a proof of concept for the treatment of acute hyperammonemia.* Gene Ther. 2015. 22: 58-64.

16. Leonard JV, et al., *The role of liver transplantation in urea cycle disorders.* Mol Genet Metab. 2004. 81 Suppl 1: S74-78.

17. Yang X, et al., *Protein O-GlcNAcylation: emerging mechanisms and functions*. Nat Rev Mol Cell Biol. 2017. 18(7):452-465.

18. Hart GW, et al., *Cycling of O-linked beta-N-acetylglucosamine on nucleocytoplasmic proteins.* Nature, 2007. 446:1017–22.

19. Hart GW, et al., *Cross talk between O-GlcNAcylation and phosphorylation: roles in signaling, transcription, and chronic disease.* Annu Rev Biochem. 2011. 80:825–58.

20. Yuzwa SA, et al., *A potent mechanism-inspired O-GlcNAcase inhibitor that blocks phosphorylation of tau in vivo.* Nat Chem Biol. 2008. 4(8):483-90.

21. Karababa A, et al., *O-GlcNAcylation as a novel ammonia-induced posttranslational protein modification in cultured rat astrocytes.* Metab Brain Dis. 2014. 29(4):975-82.

22. Bond MR, et al., *A little sugar goes a long way: the cell biology of O-GlcNAc.* J Cell Biol. 2015. 208(7):869-80.

23. Blair FN, et al., *Urea cycle disorders: a life-threatening yet treatable cause of metabolic encephalopathy in adults.* Pract Neurol. 2015. 15: 45-48.

24. Vetrini F, et al., *Gene therapy with helper-dependent adenoviral vectors: current advances and future perspectives.* Viruses, 2010. *2(9):1886-917.*

25. Brunetti-Pierri N, et al., *Helper-dependent adenoviral vectors for liver-directed gene therapy.* Hum Mol Genet. 2011. 20(R1): R7–13.

26. Brunetti-Pierri N, et al., *Transgene Expression up to 7 Years in Nonhuman Primates Following Hepatic Transduction with Helper-Dependent Adenoviral Vectors.* Hum Gene Ther., 2013. 24(8):761–5.

27. Castello R, et al., *Helper-dependent adenoviral vectors for liver-directed gene therapy of primary hyperoxaluria type 1.* Gene Ther. 2016. 23(2):129-34.

28. Brunetti-Pierri N, et al., *Improved hepatic transduction, reduced systemic vector dissemination, and long-term transgene expression by delivering helper-dependent adenoviral vectors into the surgically isolated liver of nonhuman primates*. Hum Gene Ther. 2006. 17(4):391–404.

29. Piccolo P, et al., *Gene therapy for inherited diseases of liver metabolism*. Hum Gene Ther. 2015. 26(4):186–92.

30. Pastore N, et al., *Gene transfer of master autophagy regulator TFEB results in clearance of toxic protein and correction of hepatic disease in alpha-1-anti-trypsin deficiency*. EMBO Mol Med. 2013. 5:397-412.

31. Schofield JP, et al., *Mice deficient in the urea-cycle enzyme, carbamoyl phosphate synthetase I, die during the early neonatal period from hyperammonemia*. Hepatology, 1999. 29(1):181-5.

32. Khoja S, et al., *Conditional disruption of hepatic carbamoyl phosphate synthetase 1 in mice results in hyperammonemia without orotic aciduria and can be corrected by liver-directed gene therapy*. Mol Genet Metab. 2018. 124(4):243-253.

33. Soria LR, et al., *Hepatic glutamine synthetase augmentation enhances ammonia detoxification.* J Inherit Metab Dis. 2019.1-8.

34. Darley-Usmar VM, et al., *Protein O-linked ß-N-acetylglucosamine: A novel effector of cardiomyocyte metabolism and function.* J Mol Cell Cardiol. 2012. 52(3): 538-549.

35. Haltiwanger R.S, et al., *Modulation of O-linked N-acetylglucosamine levels on nuclear and cytoplasmic proteins in vivo using the peptide O-GlcNAc-β-N-acetylglucosaminidase inhibitor O-(2-acetamido-2-deoxy-D-glucopyranosylidene) amino-N-phenylcarbamate.* J. Biol. Chem. 1998. 273, 3611–3617.

36. Ding N, et al., *Thiamet-G-mediated inhibition of O-GlcNAcase sensitizes human leukemia cells to microtubule-stabilizing agent paclitaxel*. Biochem Biophys Res Commun. 2014. 24;453(3):392-7.

37. Soria LR, et al., *Enhancement of hepatic autophagy increases ureagenesis and protects against hyperammonemia.* Proc Natl Acad Sci U S A, 2018. 9;115(2):391-396.

38. Ye X, et al., *Adenovirus-mediated in vivo gene transfer rapidly protects ornithine transcarbamylase-deficient mice from an ammonium challenge.* Pediatr Res. 1997. 41:527–534.

39. Nandi A, et al., *Global identification of O-GlcNAc-modified proteins.* Anal Chem. 2006. 15;78(2):452-8.

40. Teo CF, et al., *Glycopeptide-specific monoclonal antibodies suggest new roles for O-GlcNAc.* Nat Chem Biol. 2010. 6(5):338-43.

41. Cao W, et al., *Discovery and confirmation of O-GlcNAcylated proteins in rat liver mitochondria by combination of mass spectrometry and immunological methods.* PLoS One, 2013. 2;8(10): e76399.

42. Liu W, et al., *AANL (Agrocybe aegerita lectin 2) is a new facile tool to probe for O-GlcNAcylation.* Glycobiology, 2018. 1;28(6):363-373.

43. De Cima S, et al., *Structure of human carbamoyl phosphate synthetase: deciphering the on/off switch of humanureagenesis.* Sci Rep. 2015. 5:16950.

44. Rao X, et al., *O-GlcNAcylation of G6PD promotes the pentose phosphate pathway and tumor growth.* Nat Commun. 2015. 24;6:8468

45. Hakvoort TB, et al., *Pivotal role of glutamine synthetase in ammonia detoxification.* Hepatology, 2017. 65:281-293.

46. An D., et al., *Systemic messenger RNA therapy as a treatment for methylmanoic acidemia.* Cell Rep, 2017. 21:3548-3558.

47. Yu M., et al., *Nanotechnology for protein delivery: Overview and perspectives.* J Control Release, 2016. 240:24-37.

48. Narain A., et al., *Cell membrane coated nanoparticles: next generation therapeutics.* Nanomedicine (Lond), 2017. 12:2677-2692.

49. Forster V., et al., *Liposome supported peritoneal dialysis for detoxification of drugs and endogenous metabolites.* Sci Transl Med, 2014. 6:258ra141.

50. Lie-Venema H., et al., *Regulation of the spatiotemporal pattern of expression of the glutamine synthetase gene.* Prog Nucleic Acid Res Mol Biol, 1998. 61:243-308.

51. Takahashi H., et al., *Inhibition of brain glutamine accumulation prevents cerebral edema in hyperammonemic rats.* Am J Physiol, 1991. 261:H825-H829.

52. Haberle J, et al., *Suggested guidelines for the diagnosis and management of urea cycle disorders.* Orphanet J Rare Dis, 2012. 7:32.

53. Summar ML, et al., *Unmasked adult-onset urea cycle disorders in the critical care setting.* Crit. Care Clinic, 2005. 21: S1-S8.

54. Palmer D, et al., *Improved system for helper-dependent adenoviral vector production.* Mol Ther, 2003. 8: 846-852.

55. Piccolo P, et al., *Down-regulation of hepatocyte nuclear factor-4α and defective zonation in livers expressing mutant Z α1-antitrypsin.* Hepatology, 2017. 66(1):124-135.